Macromolecules

Editors' Choice
Open Access

pubs.acs.org/Macromolecules

Perspective

Topology Matters: Conformation and Microscopic Dynamics of Ring Polymers

Margarita Kruteva,* Jürgen Allgaier, and Dieter Richter

Cite This: *Macromolecules* 2023, 56, 7203−7229

Read Online

ACCESS | Metrics & More | Article Recommendations

ABSTRACT: Ring polymers have fascinated theorists, simulators, and experimentalists as they are the simplest polymer without ends, giving rise to important topology related properties. We present the state of the art of recent synthetic efforts and investigations into the structure and dynamics of dense nonconcatenated ring polymer systems. Analyzing the existing knowledge, we identify challenges for future research: In the realm of synthesis the creation of well-defined high molecular weight rings based on different monomers are highly desirable. In the field of ring conformations, the existence of double folded structures that are at the basis of many theoretical approaches was severely challenged and further scrutiny is needed. Similarly, the issue of the size dependent transition to mass fractal structures, or the effect of local stiffness on the conformation and dynamics are open questions. The role of ring−ring threading in the terminal dynamics of rings needs to be further elucidated. In particular, the novel proposed topological glass transition for very high molecular weight ring melts awaits experimental verification. Experimentally, ring-linear blends are very seldomly investigated: only a small number of studies on the miscibility and the conformation of rings in such blends are available. Microscopic experiments on the dynamics are nearly entirely missing. Finally, as different theoretical approaches are always backed by corresponding simulations, a crucial task would be to find out how the different approaches connect to each other and which experiments should be performed.

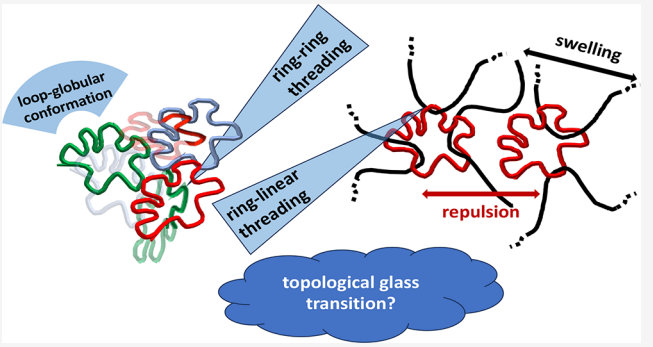

1. INTRODUCTION

Polymeric liquids display a multitude of fascinating properties that to a large extent relate to their huge number of internal degrees of freedom and variety of architectures (linear, branched, ring, etc). In the melt of linear polymers (LP) the mutual interaction is screened, and the LP conformation assumes a Gaussian Random Walk, while the chain dynamics is governed by reptation—long mutually interpenetrating LP confine each other in tubes around their coarse-grained profile: The polymer relaxation takes place in creeping out of the confining tubes by the chain ends. This famous reptation concept is supported by numerous experiments including rheology[1] and microscopic neutron spin echo (NSE) investigations.[2] The viscoelastic properties at intermediate times are rubber-like with a plateau modulus related to the tube step length. For branched systems, strands have to fold back, in order to find a new conformation without crossing any other chain, resulting in an exponential growth of the longest relaxation time due to the entropy barrier between different states.[3,4]

Interestingly ring polymers were first detected in the realm of biology, where e.g., the DNA in the genome forms cyclic structures.[5] Chromatin fibers are packed at a reasonably high density like a melt of linear chains; However, the different chromosomes in the nucleus do not intermix, but instead segregate in stable territories as the ring conformations in a melt. Also, various cyclic peptides have been found from plants and bacteria which exhibit enhanced stability against heating and degradation compared to their linear counterparts.[6]

The noncrossing requirement in nonconcatenated ring polymers creates topological constraints, which impose important restrictions on the phase space of the system. For ring polymers interpenetration is costly entropically and compact structures evolve for high molecular weights—ring polymers are assumed to become mass fractals confining rings into territories. Grosberg hypothesized that the equilibrium state of nonconcatenated ring polymers in the melt is a crumpled globule; each subchain condenses on itself with the result that the polymer backbone is self-similar to a fractal dimension of 3.[7] Cates and Deutsch proposed that nonconcatenated rings in the melt may exhibit statistics intermediate between those of

Received: March 28, 2023
Revised: July 23, 2023
Published: September 2, 2023

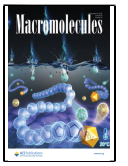

https://doi.org/10.1021/acs.macromol.3c00560
Macromolecules 2023, 56, 7203−7229

collapsed ($\nu = 1/3$) and Gaussian ($\nu = 1/2$) chains.[8] On the basis of a Flory type mean field theory they conjectured on a scaling exponent $\nu = 2/5$. Numerical simulations appeared to support this conjecture but recent simulations claimed a mass fractal statistics $\nu = 1/3$ for sufficiently long rings[9−13] suggesting an interesting relation between polymer topology and biologically important problems such as the formation of the chromosome territories.[14] Finally, Halverson et al. provided coarse grained MD simulations on the conformation of cyclic polymers with the so far largest size up to 57 N/N_e, where N_e denotes the entanglement distance of the corresponding linear chain.[15] These simulations indicate the crossover to mass fractal behavior.[16]

Other than the dynamics of linear or branched chains that predominantly takes place via the chain ends, rings do not feature ends and their dynamics is considered to be self-similar and thus fundamentally different from those of chains displaying ends with the consequence that, e.g., the dynamic modulus of a ring melt does not exhibit a plateau regime but instead displays a power law relaxation.[17] For the internal dynamics of a self-similar ring polymer Grosberg derived a terminal relaxation time $\tau_d \approx \tau_e(N/N_{e,0})^{2.56}$, where τ_e is relaxation time of an entanglement strand and $N_{e,0}$ is an elementary loop size that relates to the entanglement strand size N_e in the corresponding linear polymer.[18] Finally in 2016 Rubinstein developed the self-consistent Fractal Loopy Globule (FLG) model, which is based on the conjecture that the overlap criterion[19,20] in the packing model for entanglements also governs the rule for overlapping loops in polymer rings. The constant overlap of loops is conjectured to occur in a self-similar way over a wide range of length scales from $N_{e,0}$ up to ring size R. The dynamics of such rings in a melt is governed by topological constraints that dilute with progressing time, because with time loops of increasing sizes are relaxed and cease to be obstacles. Recently, combining results of SANS[21] with PFG-NMR and NSE the unique topology driven self-similar ring dynamics predicted by the FLG model could be verified experimentally.[22]

Aside of the power law relaxation the dynamic modulus of ring melts displays a very slow tail that is ascribed to ring−ring threadings, which exhibit relaxation times much longer than those of the internal ring relaxations. Simulations have revealed multiple threading events with their relative number increasing with the ring M_w.[23,24] Simulations by Michieletto and Turner suggest that these threadings for large rings may immobilize the melt and induce a novel topological glass transition.[25] Finally, by analogy of ring systems with soft colloids Sakaue introduced the concept of a topological volume that allows to estimate the large scale collective dynamics of dense ring systems.[26,27] From the experimental side also a possible role of linear contaminants was brought forward.[17]

Another open field is the structure and dynamics of ring−linear blends: There, threading events between rings and linear components to a large extend are expected to govern the dynamic properties such as COM diffusion. Tsalikis and Mavrantzas by atomistic simulation investigated the threading phenomenon on ring-linear PEO blends.[28] For higher M_w the occurrence of multiple threading events was evidenced. The threading dynamics, thereby, is slow: a linear molecule threading a cyclic one may need times up to an order of magnitude longer than the longest ring relaxation time to fully pass through the ring. Unexpectedly Kruteva et al. observed two distinctly different diffusion modes for dilute large rings in a highly entangled linear host;[29] a phenomenon that still waits for an explanation. Gooßen et al. by NSE found evidence that dilute rings immersed in a highly entangled linear host sense the entanglement dynamics of the host.[30]

Other than for linear polymers many facets of ring structure and dynamics are still mysterious: e.g., are lattice trees good models for rings in the melt? Does the delayed terminal relaxation relate to ring−ring threading? And does such threading possibly induce a topological glass transition. In this perspective paper we survey recent progress in the understanding of dense polymer ring systems with the goal to identify open questions and future directions emphasizing thereby, fundamental aspects. We begin with the current status of polymer ring synthesis underscoring the need for novel routes toward well-defined large ring molecules based on a variety of different monomers. Then we focus on the ring conformation presenting theoretical, simulation and experimental results. The next part deals with the dynamics of pure ring systems discussing theoretical approaches, large scale simulations and experimental results on large ring systems; the issue of threading is particularly emphasized. In particular, we address the dynamics of ring-linear blends, where ring-linear threadings are governing the dynamics. In the following section we discuss the idea of a topological glass transition, which is proposed based on MD simulations. Unfortunately, microscopic experiments are still missing. In the last part we wrap up and summarize the most important challenges and perspectives for future work.

2. SYNTHESIS

In order to study structural and dynamic properties of ring polymers, samples of high structural purity are required which exhibit narrow molecular weight distributions (MWDs). In addition, it must be possible to predetermine M_w. Especially rheological studies require a broad range of different M_w up to long chains where the linear analogs are highly entangled. Depending on the technique used, the required sample quantities are usually within the 100 mg to gram range.

In the past decades a huge number of different techniques was developed for the synthesis of ring-shaped polymers covering a large variety of different monomers. Mainly two synthetic strategies were employed: the ring closure technique and the ring expansion technique[31−41] (Figure 1). In the ring closure approach, first linear precursors are synthesized using living or

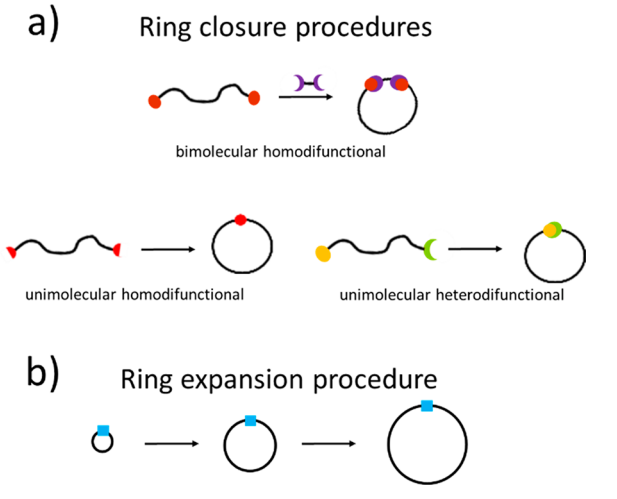

Figure 1. Synthetic pathways for the production of ring polymers: (a) ring closure technique, (b) ring expansion technique.

https://doi.org/10.1021/acs.macromol.3c00560
Macromolecules 2023, 56, 7203−7229

controlled polymerization techniques, which also allow for equipping the chain ends with functional groups. Depending on the nature of the end groups, unimolecular or bimolecular strategies are used for the following cyclization step (Figure 1a). The ring expansion technique follows a completely different strategy. Here monomers are continuously inserted into a ring low M_w initiator molecule (Figure 1b). Most of the model ring polymers used for the study of fundamental physical properties were synthesized using the ring closure procedure. Therefore, in this chapter we will mainly focus on this technique.

Anionic polymerization techniques were among the first ones used for the ring closure approach. Styrene and diene monomers were polymerized with difunctional initiators and the subsequent reaction of the carbanionic head groups with difunctional chlorosilane agents yielded the ring products.[42,43] Generally, the polymerization of styrene and diene monomers with lithium organic initiators exhibits a very low degree of termination reactions in nonpolar solvents and the reaction of lithium organic head groups with chlorosilane agents are basically free of side reactions. However, difunctional initiators have low solubility especially in hydrocarbon solvents and initiation processes are slow, leading to somewhat broader MWDs of the resulting linear precursors. Therefore, in later studies protected initiators were used for the polymerization processes in combination with a large variety of different linking approaches for the cyclization reactions.[44−48] By means of a different strategy, styrene was polymerized with a vinyl functionalized lithium organic initiator. The living chains were dimerized with a dichlororosilane linker and the metathesis cyclization reaction was performed with a Grubbs catalyst. As nondimerized polystyrene chains were functionalized with OH-groups after the dimerization step, linear byproducts could easily be eliminated in a simple chromatography procedure.[49] For the synthesis of ring polylactides, first a linear α-azide-ω-alkyne precursor was produced by polymerizing the lactide monomer using an azide functionalized alcohol initiator and converting the alcohol end group into an alkyne functionality. Azide−alkyne click chemistry was used in the following step for the ring closure reaction.[50]

Besides a large variety of other techniques, the anionic ring opening polymerization of epoxides is of relevance for the synthesis of ring model polymers. By means of functional initiators, heterodifunctional ring closure reactions can be applied.[51] Using ethylene oxide as monomer, very simple ring closure chemistries are possible as the use of diol initiators yields poly(ethylene glycol)s (PEGs) which by nature contain two alcohol end groups. These functionalities can be used for the cyclization reaction.[44,52−54] In an approach to increase product yield, the cyclization reaction of PEG was carried out on a high concentration level.[55] As a consequence, visible amounts of mainly linear unimeric and chain extended side products were present in the reaction mixtures (Fugure 2). For the removal of linear chains, a process was developed which comprised the quantitative oxidation of alcoholic PEG chain ends to carboxylic acid groups and their subsequent removal using a basic ion-exchange resin. As a result, ring PEG was obtained in high structural purity up to a M_w of 20 kg/mol in quantities of several grams. The method was later improved by using a more efficient ion-exchange resin and carrying out the polymerization with a protected initiator.[56] This allowed applying the more efficient heterodifunctional pathway for the ring closure reaction. As a result, the M_w range could be extended to 100 kg/mol.

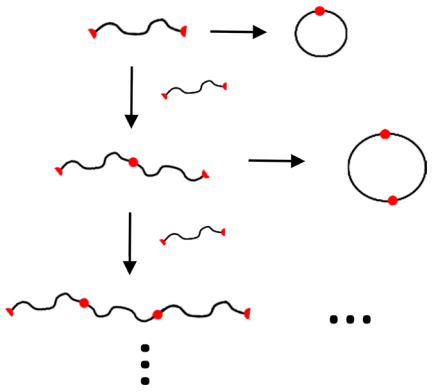

Figure 2. Chain extended side products being formed during the ring closure reaction of the linear precursor.

Besides anionic polymerization techniques mainly controlled radical processes were employed for the polymerization of a multitude of different monomers. This technique allows one to very efficiently to carry out the cyclization reaction as there is a huge variety of available end groups and the polymer chains can be equipped with different functionalities, directly reacting in a heterodifunctional ring closure pathway (Figure 1). Many of the cyclization reactions are based on azide/alkyne or thiol/ene click reactions[57−63] but also other ring closure reactions were used.[64−66]

In ring expansion polymerization processes ring monomers are incorporated into a ring molecule, which contains a weak covalent or noncovalent bond. In the past years, a huge variety of different strategies were developed. One of the most promising ones is based on the metathesis polymerization of ring alkenes. This procedure was pioneered by Grubbs et al.[67] Later this strategy was used to synthesize a variety of other ring polymers.[68−72] A different technique based on zwitterionic reaction centers was applied to synthesize macrocycles out of low M_w ring esters but also other monomers.[36,73−77]

Ring expansion polymerization represents a very powerful possibility for the synthesis of ring polymers as the ring structure exists from the beginning and there is no entropic loss for the ring closure reaction. In addition, high molecular weights are accessible and large sample quantities can be obtained as it is possible to perform the polymerization reactions at high concentrations. However, the polymerization techniques used for the ring expansion approach usually result in polymers with broader MWDs. The coexistence of linear chains in the ring products is difficult to check, which is particularly the case for high M_w. However, detailed physical studies rely on precise M_w, narrow MWDs and low contents of contamination with linear chains. This is especially of importance for rheological studies, where both experimental and simulation results show that already small quantities of linear impurities strongly influence the behavior of ring polymers.[16,17,78,79]

These requirements are more fulfilled for the ring closure processes, where living and controlled polymerization techniques are employed. As a result, the linear precursor polymers have narrow MWDs and the M_w can be predetermined. In addition, these polymerization procedures allow for equipping the chain ends with the desired functionalities for the following ring closure reaction. Among the polymerization techniques used for ring closure procedures, controlled radical techniques are very powerful as the end groups can be equipped with a wide variety of different functionalities for the ring closure reaction.

https://doi.org/10.1021/acs.macromol.3c00560
Macromolecules 2023, 56, 7203−7229

However, the controlled radical processes are largely limited to smaller M_w as the radical nature of the polymerization event causes termination reactions, leading to nonfunctional chain ends and as a consequence thereof to incomplete ring formation. By nature, the termination reactions get more prominent with increasing chain length. Anionic polymerization techniques, however, are restricted to a limited number of monomers and functional initiators, but higher polymerization degrees are accessible compared to the controlled radical procedures. This is especially the case for styrene, diene, and ethylene oxide. For these monomers, polymerization degrees of 10 000 and more are possible with still narrow MWDs. In addition, 1,4-polydienes and PEG possess small entanglement M_w so that ring polymers are accessible where the linear analogs are highly entangled.

A drawback of the ring closure procedure is the limited sample quantity, which usually is more in the milligram than the gram quantity. The reason for this is that the ring closure reaction is always accompanied by the reaction of chain ends of two different chains, leading to higher M_w chain extended products (Figure 2). The latter reaction can be minimized by carrying out the ring closure at high dilution. For practical reasons, this results in small sample quantities.

A possible way out of this dilemma is to perform the ring closure reaction at higher concentration and to remove inevitable side products in a subsequent purification step. Here especially the linear chain extended molecules and in that case the mother compound has to be considered.[55] Chain extended ring molecules play a minor role as the probability for the ring closure reaction is strongly reduced with increasing chain length.[80] Purification steps also may be necessary if a high structural purity of the product is required, especially for high M_w. However, separating the different structures is challenging because of the largely similar chemical and physical properties of the different architectures. So far liquid chromatography procedures[81−83] and liquid chromatography in combination with other methods[48] have been used successfully to separate ring and linear chains in smaller quantities. In the future also other techniques might be used, which are based on other differences between linear and ring structures.[84] Especially the postring closure chemical modification of the end groups of remaining linear chains is a powerful tool to increase the difference between ring and linear chains and to separate also larger sample quantities.[49,55]

It should be emphasized that not only new and improved synthetic procedures for ring polymers are of relevance but also the analytical characterization is a key element in this research field. Usually, the analysis task gets more difficult with increasing M_w of the polymer. For lower M_w MALDI-TOF mass spectrometry is very a powerful analysis technique. It allows one to prove the ring formation and to identify possible linear side products on a qualitative or semiquantitative scale. The method, however, loses its advantages for high M_w due to the loss of resolution power. Size exclusion chromatography (SEC), however, is of limited use because of the small separation efficiency between ring and linear architectures.[85] Therefore, the detection of smaller quantities of linear material is normally not possible using SEC. Liquid chromatography at the critical condition (LCCC) has proven to be the most powerful method for the precise analysis of ring polymers due to its superior resolution power in separating cycles from linear structures.[85−88] However, this method is by far more complex in the use as a routine method compared to SEC. Besides chromatography techniques, proton NMR can be used to detect linear contaminants if end-group signals can be separated from the other polymer signals.[55] Again, this method is limited to M_w up to a few 10 kg/mol. Especially if the fraction of linear chains is in the percent or even subpercent range, the end group signals become so small that even powerful NMR instruments in combination with extended measurement times do not allow resolving these signals.

In order to improve the availability of cyclic polymers for physical experiments, it is important to have access to cyclic samples up to high M_w, where the linear analog is well entangled. The needed M_w can be minimized if polymers with small M_e are used. This is especially the case for PEG and 1,4-polybtadiene (1,4-PB), both having entanglement molecular weights of 2 kg/mol. 1,4-PB is of particular interest due to its low glass transition temperature of about −80 °C, which makes it a useful material for rheological experiments. Besides polymer properties and accessible M_w, sample quantities are of high relevance from the practical standpoint. For many physical experiments sample quantities in the gram scale are needed. However, if the ring closure reaction is carried out at high dilution, only substantially smaller quantities are accessible. Therefore, alternative procedures are needed, where the ring closure reaction takes place at higher concentration. Such procedures require purification steps to remove chain-extended byproducts. Liquid chromatography techniques can be very useful for this purpose. But due to small sample quantities automated processes are required to repeat the experiment many times. Alternatively, chain-end refunctionalization of the linear byproducts with subsequent separation processes might be applied. It is obvious, that with increasing chain length such procedures get more challenging. So far for 1,4-PB the outlined processes are still missing but would be a significant step forward for the physical investigation of cyclic polymers.

Finally, we like to give an example. In order to get rid of the final residual contamination the Jülich group[56] applied ion exchange chromatography. There the unreacted chain ends are oxidized yielding a carbonic acid terminal group that reacts with the walls of the column. The remaining pure rings are washed out. To demonstrate the accomplished purity, the SEC chromatogram in Figure 3 compares the purified 100 kg/mol

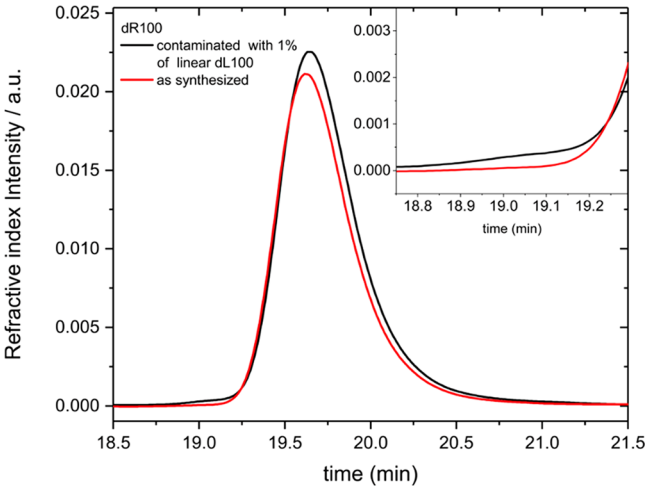

Figure 3. SEC chromatograms of the 100 K deuterated ring with and without of 1% linear 100 kg/mol material. The inset magnifies the region between 18.7 and 19.4 min elution time.[56] Reproduced with permission from ref 56. Copyright 2021 AIP Publishing.

https://doi.org/10.1021/acs.macromol.3c00560
Macromolecules 2023, 56, 7203−7229

ring with the same ring, where 1% 100 kg/mol linear contamination was added. The inset shows the difference between the traces—1% contamination can be clearly distinguished and safely excluded.

3. RING CONFORMATION

Polymer macromolecules have a hierarchical structure characterized by several regions where different interactions play a role. On the segmental level the short-range interactions between the neighboring segments or solvent molecules determine the local structure of the polymer chain. On the larger scale the connected segments can interact through topological long-living interactions. The topological interactions are especially important for ring polymers: compared to linear polymers that easily interpenetrate, the nonconcatenation constraint goes along with entropic penalties that make interpenetration costly. A consequence of the specific topological interactions is threading of a ring by neighbors that is in particular important for the blends of rings with the other topologies, e.g., linear or branched polymer chains. Due to the synthesis limitations, only a few experimental works on the conformation of ring polymers are known. Mainly they are represented by small angle neutron scattering (SANS).

3.1. Pure Ring Conformation. *3.1.1. Theory.* Over the years several theories were suggested to describe the multiscale conformation of ring polymers.[7,8,18,26,27,89−95] Ring conformations were described in terms of tree-like models also reflecting a globular structure that takes into account effects of topological constraints. We will describe the existing theories in chronological order.

Although not related to the specific ring conformation, the scaling ideas based on self-similarity were quite important for the further development of theoretical approaches for the ring conformation. The *double folded lattice animal* (DFLA) model of a ring suggested by Rubinstein considers randomly branched double folded loops that maximize entropy.[92] The model leads to a fractal dimension $d_f = 4$ and considers branching between fixed obstacles (Figure 4).

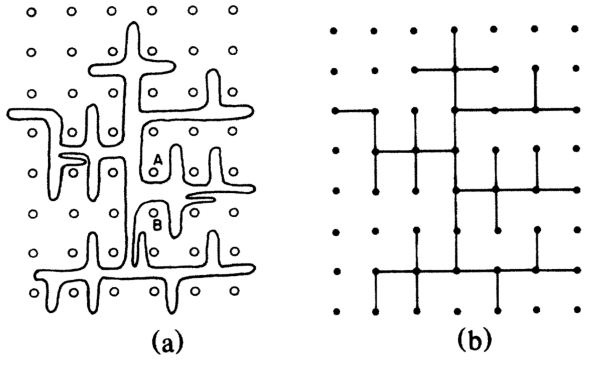

Figure 4. (a) Ring polymer in a gel can be mapped onto (b) a lattice tree on a dual lattice.[92] Reproduced with permission from ref 92. Copyright 1986 American Physical Society.

In parallel with Rubinstein's scaling model Cates and Deutsch (CD) made conjectures concerning the equilibrium statistics of ring polymers based on a *mean field theory*.[8] They calculated the free energy cost of topological interactions from the balance between the topological free energy taken as proportional to the overlap parameter O_{CD}: $k_BTO_{CD} \approx k_BTR^3/Nv_0$ with the free energy penalty due to constraints: k_BTNl^2/R^2. Minimization leads to ring size $R \sim N^{2/5}$ or $d_f = 2.5$ (N: overall chain length; v_0: monomer volume, l: monomer length). Suzuki et al. modified the *mean field theory* in three dimensions.[94] Free energy per ring in the melt was estimated from the consideration of an osmotic pressure due to neighboring molecules instead of using the overlap parameter and an entropic penalty of polymer chain conformations. The modified *mean field theory* predicts $R \sim N^{1/3}$. Bond fluctuation model (BFM) simulation results are consistent with the *mean field theory*: The fractal exponent ν decreases gradually with increasing N, and finally it reaches the limiting value, 1/3, in the range of $N > 1536$, i.e., $R \sim N^{1/3}$.

However, for the accessible range of N, where $R \sim N^{2/5}$ is observed, it was shown by several works[90,96] that the number of concatenations among rings grows linearly with N, when rings are allowed to freely penetrate each other. Since these concatenated states are the states that have to be kicked out for nonconcatenated ring melts, the penalty for nonconcatenation must scale accordingly. Thus, the first term for the topological free energy is wrong in the CD model. Also, the second term is not correct since three-body interactions should stabilize the compression of the rings as proposed by Sakaue[93] and Lang et al.[90] Thus, both terms in the CD model are known to be incorrect. This relates also to later works basing on the CD theory.

Sakaue described the topological constraints in terms of an *excluded volume concept* called the *topological volume*.[27] He predicted a broad crossover of the ring conformation toward a globular state. The onset of compact statistics was estimated to occur around $N^* \approx 10\, N_e$. This conformation change was related to a topological phase transition and a topological glassy state—both phenomena will be considered in the following chapters.

Quantitative estimations of the ring conformations are presented in a later manuscript by Sakaue that introduces a number of different topological regimes inducing various conformations.[93] First of all the presence of (i) an intrinsic topological length scale $N_1 \approx N_e$ is assumed which signals the onset of the topological effect—rings smaller than N_1 in the melt display Gaussian statistics; (ii) the characteristic length or topological mesh $\xi(N_1) = l_{seg}N_1^{1/2}$ increases in a broad transition regime with the ring length N as $\xi(N) \sim N^{1/5}$ until the compact mass fractal state at N_2 is reached. (iii) in the broad transition regime the radius of gyration follows a power law $R_g \sim N^{\nu_{eff}}$ with $\nu_{eff} = 0.4$ very close to the CD conjecture.[8] Note that Sakaue proposes an N-dependent elementary loop size $\xi(N)$. The geometrical behavior of the ring dimension is related to the number of ring neighbors N_R that increases from about 6 at N_1 to in the order of 15 at the onset of compact statistics realized at N_2.

The DFLA model was generalized by Grosberg, allowing for overlapping of loops.[18] The ring conformation underlies a skeleton lattice tree that branches randomly at the entanglement spacing $d_{tube} \cong l\sqrt{N_e}$ where $l = l_0\sqrt{C_\infty n_b}$ is the monomer length (n_b: number of main chain bonds in a monomer, C_∞: the characteristic ratio l_0: bond length). In addition to the randomly branched statistics assumed by Rubinstein[92] the backbone primitive path was considered as a self-avoiding random walk. Thus, the free energy becomes a function of the backbone length L of the lattice tree with a statistic following a self-avoiding random walk with a fractal dimension $d_b = 5/3$ and for the whole ring $d_f = 3$. For the DFLA model $d_b = 2$ and $d_f = 4$ was found.

Obukhov considered rings as a collection of Gaussian loops ranging from $N_{e,0}$ to the size of the backbone $L \sim N^{2/3}$ that are assembled in random trees.[91] The so-called decorated loop

https://doi.org/10.1021/acs.macromol.3c00560
Macromolecules 2023, 56, 7203−7229

model is based on a geometrical description of the ring structure and for the radius of gyration R_g predicts:

$$R_g^2 \cong 1.6R_{e,0}^2\left(\frac{N}{N_{e,0}}\right)^{2/3}\left[1 - 0.38\left(\frac{N}{N_{e,0}}\right)^{-1/3}\right] \quad (1)$$

where $N_{e,0} \cong N_e$ and $R_{e,0}^2 = l^2 N_{e,0}/12$ the size of the elementary loop. Equation 1 describes a very slow crossover to the asymptotic $d_f = 3$ mass fractal.

Kavassalis and Noolandi suggested that a minimum number of different linear chains (∼20) must overlap in a volume, called entanglement volume, in order to create an entanglement—entanglements relate to chain packing.[19] This overlap criterion was used by Ge et al. in order to describe ring conformations.[95] They developed the Fractal Loopy Globule (FLG) model, assuming the overlap parameter $O_{KN} \cong l^3 N_e^{1/2}/\nu_0 \approx 20$ verified for numerous linear polymer melts in terms of the packing model[20] also governs the loop overlap in ring systems. Following the overlapping criterion, ring conformations consist of large loops that obeying the overlap criterion O_{KN} with similar sized loops of neighboring rings, and a set of smaller loops (Figure 5).

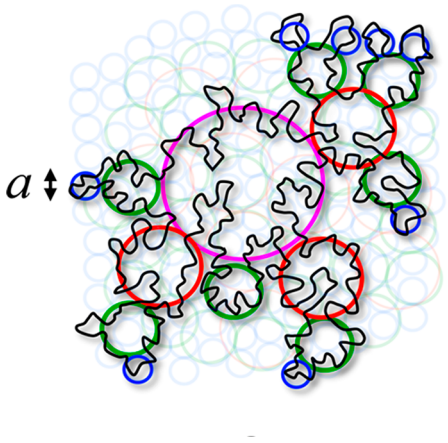

Figure 5. Schematic sketch of the fractal loopy globule (FLG) conformation of a ring (black line) in a melt of nonconcatenated rings. Regular circles of different colors indicate the length scales where loops of various sizes overlap with similar size neighbors at the same overlap parameter O_{KN}. Circles associated with other rings are shown as the dimmed background. $a \equiv R_{e,0}$ is the size of the elementary loop.[95] Reproduced with permission from ref 95. Copyright 2016 American Chemical Society.

The constant overlap of loops is conjectured to occur in a self-similar way over a wide range of length scales from the entanglement length $d_{tube} = l\sqrt{N_{e,0}}$ up to the ring size $(O_{KN}Nv_0)^{1/3}$. It is pointed out that the description of loop overlaps on all length scales using O_{KN} is a conjecture and need to be studied by experimental methods and simulations.

Motivated by simulation works, Dell et al. adopted a two-fractal exponent ring model for the intramolecular structure factor.[89] At smaller length scales a ring behaves as a linear chain, while on larger scales it corresponds to a space-feeling object with a fractal dimension $d_f = d_s = 3$. The crossover between these two regimes is related to the entanglement length of the linear chain analog. The number of nearest neighbor rings increases at small N, akin to linear chain melts, but then tends to saturate at large N, in accord with simulations. The model was initially developed for soft suspensions and does not consider effects specific for the rings, e.g., threading. It is based on a well-established philosophy: construct minimalistic coarse-grained polymer models and use them in conjunction with liquid state polymeric integral equation theory at the segmental level, to predict the equilibrium collective and intermolecular packing structure of dense fluids of globules and nonconcatenated ring polymers. The authors suppose that this theoretical approach can be used to describe the behavior of other complex fluids composed of soft partially interpenetrating objects such as core—shell microgels and nanogels, hairy colloids, and highly branched dendritic nanoparticles.

3.1.2. Computer Simulations. Ring conformations have been subject of numerous simulations including atomistic molecular dynamics (MD) simulations and larger scale coarse-grained approaches. Mainly they focused on nonconcatenated unknotted rings and some of them emphasized the similarity to packing of chromatin in the nucleus.[97] Depending on the applied simulation technique, the details of the single ring conformation, e.g., the form factor, and interactions between the neighboring rings at high concentrations were elucidated. In this way double-folding on branched or tree-like conformations, self-similarity, threadings, and entanglements on different length scales are discussed. Finally, the simulations support the theoretical prediction of a topological glassy state and conditions for topological phase transitions described in the chapter "Topological Glass Transition".

Halverson et al. rescaled many simulation results in terms of $N/N_{e,0}$, resulting in a master curve combining all results for the ring size R_g (Figure 6).[16] They found a common crossover from

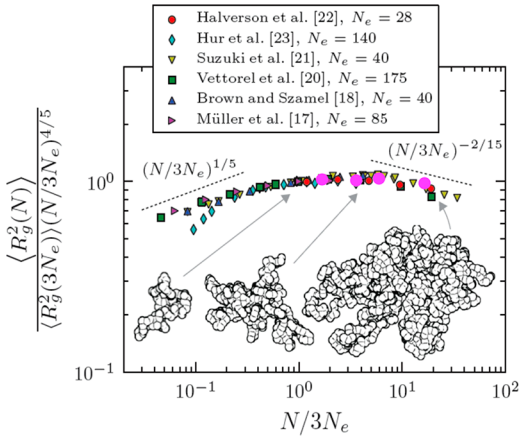

Figure 6. Dependence of the ring R_g^2 on the reduced chain length. For the references to the other simulation and experimental data see the original paper.[16] Note that $N_e = N_{e,0}$. The large magenta circles indicate the experimental values obtained by SANS.[56] Reproduced with permission from ref 16. Copyright 2012 American Physical Society.

$R \sim N^{2/5}$ in the intermediate regime to mass fractal behavior $R \sim N^{1/3}$ at around $N/N_{e,0} \cong 15$. Coarse-grained molecular dynamics (MD) studies on the static properties of a melt of nonconcatenated rings show that the ring dimension appears to approach a $N^{1/3}$ power law. At that the ring conformations are far from trivial: the simulations demonstrate significant mutual interpenetration. Moreover, the entropic barrier to form large open loops is small and therefore the larger loops are frequently observed.[15]

From a primitive path analysis of the MD simulation results by Halverson et al.,[15] Ge et al. arrived at a crossover for the characteristic size of the primitive path segment to $d_f = 3$ as a

https://doi.org/10.1021/acs.macromol.3c00560
Macromolecules 2023, 56, 7203−7229

function of the reduced contour length.[95] Simulations by Rosa and Everaers support Rubinstein's conjecture[92] and find strong evidence for the scenario that rings crumple by adopting lattice tree-like ribbon structures characterized by randomly branched looping on the entanglement scale.[98] Using their multiscale approach, they were able to show that melts of rings of total contour length L_r can be quantitatively mapped onto melts of interacting lattice trees with gyration radii $R_g^2(L_r) \sim L_r^{2\nu}$ and $\nu = 0.32 \pm 0.01$.

Atomistic MD simulations of polyethylene performed by Jeong and Douglas led to the conclusion that the excluded volume interactions in the ring melt are not screened as in the case of linear polymers. For large rings $N > 7\ N_{e,0}$ their shape resembles percolation clusters of branched structures.[99] As a measure for the changed shape the average principal eigenvalues of the gyration tensor are considered. Another MD simulation performed on polyethylene rings report $R \sim N^{2/5}$ which reproduces Halverson's results for the intermediate regime.[100] Apparently, the mass fractal behavior has yet not been reached.

Mavrantzas et al. performed atomistic MD simulations of poly(ethylene oxide) rings with a molecular weight of $M_w \sim 10\ M_e$, where M_e is the entanglement molecular weight.[101] Their predictions for the mean squared radius of gyration $\langle R_g^2 \rangle$ of rings in the melt are described remarkably well by the decorated loop model proposed by Obukhov et al.[91] The molecular weight dependence of macroscopic properties, i.e., viscosity and COM diffusion, demonstrate a crossover at $M_w \sim M_e$. For larger rings the authors found a COM diffusion coefficient and a viscosity scaling as $D \sim M_w^{-2}$ and $\eta \sim M_w^{1.9}$, respectively. These findings compare well with a number of experimental works studying corresponding ring sizes. However, the ring sizes investigated seem to be not large enough for a quantitative estimation of the molecular weight dependence.

Monte Carlo simulations of ring in solution allowed to find the scaling relationship between the concentration dependence and the chain-length dependence of the radius of gyration. In limiting case of a melt, Reigh and Yoon obtain $\langle R_g^2 \rangle \sim N^{0.72}$, indicating highly collapsed conformations for long-chain ring polymers in the melt.[102]

On the basis of Monte Carlo simulations of ring melts with different bending rigidities Rosa et al. were able to separate threading from branching of unknotted and nonconcatenated rings in melt. They reported that rings are double-folded, even more strongly for stiffer rings, on and above the entanglement length scale, while the threadings are localized on smaller scales.[96] Such effects influence strongly the dynamics and will be discussed in the chapter "Ring dynamics".

The Bond Fluctuation Model (BFM) was used by Lang et al. to study the role of topology on the ring dynamics as a function of ring size and concentration.[90] They spanned the concentration range from a solution of entangled nonconcatenated rings (diluted solution) to interpenetrating rings (melt) and found different regimes for the conformation. The number of nonconcatenated conformations allowed in a melt of concatenated rings was counted. These allowed conformations were found to decay exponentially with the area bound by a ring polymer. According to the authors from this observation an estimation of the entropic penalty for nonconcatenation could be obtained. For the intermediate regimes the scaling of the ring sizes $R \sim N^{2/5}$ resulted from balancing nonconcatenation with weak compression of rings. For larger rings the power law regime changes to $R \sim N^{3/8}$, where nonconcatenation and strong compression are implied.

The properties of ring polymers under confinement are largely unexplored. A pioneering coarse-grained simulation investigated the conformation of ring polymer melts under planar confinement.[103] The authors found that the architectural difference between ring and linear polymers has no effect on the monomer-scale packing close to the wall (Figure 7a). Normalized COM densities analyzed for the rings of different sizes indicate that the ring polymers are less compressed in the direction normal to the walls (Figure 7b). Figure 7c indicates that the confined rings tend to separate and form territories (Figure 7c). The COM densities (Figure 7b) are discussed in terms of the correlation hole effect found by simulations for linear polymers under 2D cylindrical confinement. For ring polymers the correlation hole effect was enhanced at these confinement conditions. Moreover, in highly confined systems, the strong correlation hole effect prevents other rings from penetrating, thus trending toward molecular segregation.

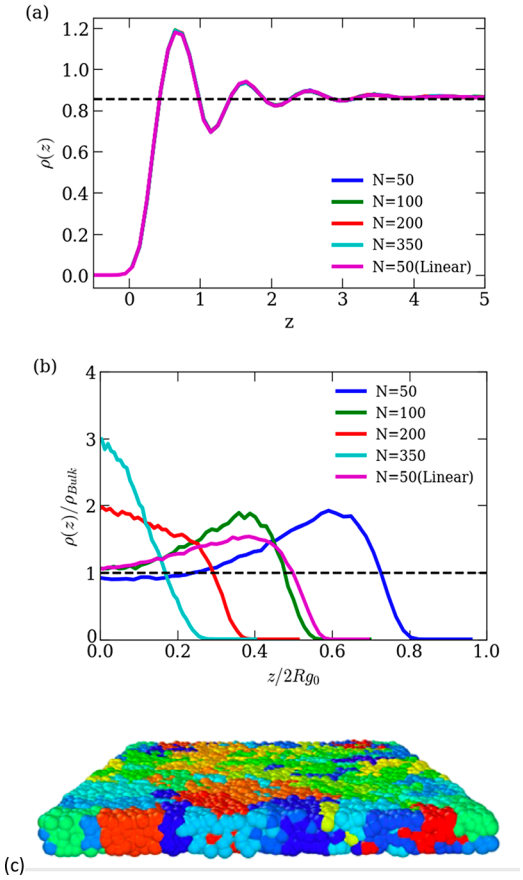

Figure 7. (a) Monomer density of ring polymers for different degrees of polymerization (N = 50, 100, 200, and 350) and linear polymers with N = 50 at the confinement thickness of $H = 10\sigma$. This film thickness corresponds to $H/2R_g$ = 1.94, 1.41, 1.05, 0.81, and 1.40 (linear), respectively. (b) Normalized COM density of ring polymers and linear polymers at the same confined situation as the monomer density plot in (a). The positions of the polymers in the confinements z are normalized by $2R_g$, where R_g is the bulk radius of gyration for each chain length and $z/2R_g = 0$ is the center of the film. (c) Rings of chain length N = 350 forming territories in thin film confinement with a thickness of $H = 5\sigma$.[103] Reproduced with permission from ref 103. Copyright 2020 AIP Publishing.

Determination of specific ring conformations at different confinement conditions might provide basic information

https://doi.org/10.1021/acs.macromol.3c00560
Macromolecules 2023, 56, 7203−7229

regarding the origin of the hypothetical topological phase transition and specific dynamical properties of the pure rings and their blends with other topologies.

3.1.3. Experiments. In general, experimental techniques allowing one to elucidate the conformations on the single ring level are limited to scattering techniques. There are a few experimental works on fluorescent microscopy allowing to measure conformation of a single labeled chain in the presence of surrounding macromolecules. These single molecule methods are mainly focused on the study of DNA molecules in solution.[90] In particular, the highly concentrated DNA solutions are used as a model system to probe entanglement properties for different topologies of ring polymers and blends of linear and ring polymers.

Depending on the contrast conditions Small Angle X-ray Scattering (SAXS) can be used to measure the conformation of polymer rings in a solvent.[104] For huge ring specimens as DNA different types of microscopies (TEM, SEM) can be applied. Main disadvantage of SAXS techniques relates to the degradation of polymers because of γ − radiation and its limitation to dilute solutions. Neutrons do not have this disadvantage and allow to study the ring conformation without damage. Furthermore, exploiting the contrast between hydrogenated and deuterated polymers Small Angle Neutron Scattering (SANS) allows to decipher the ring conformation even in dense ring systems. In earlier works of the Higgins' group ring poly(dimethylsiloxane) (PDMS) melts were studied by SANS.[105] It has been shown that rings in the melt are partially collapsed compared to linear chains obeying a gyration radii dependence $R_g \sim N^{0.4}$ in agreement with simulations and theories (see e.g., ref105). Detailed analysis of the SANS scattering functions demonstrated that the Debye equation[106] cannot describe the ring scattering function, at least up to $M_w <$ 10 kg/mol.[107] The Casassa form factor was found to give a better representation of the SANS data[108]

$$P(Q) = \left(\frac{2}{\sqrt{t}}\right)\exp\left(-\frac{t}{4}\right)\int_0^{t^{1/2}/2}\exp(x^2)\mathrm{d}x = \left(\frac{2}{\sqrt{t}}\right)\mathrm{Dw}\left(\frac{\sqrt{t}}{2}\right) \quad (2)$$

where $t = Q^2R_g^2$ and $\mathrm{Dw}(x)$ is the Dawson integral. The authors show that this function which was initially developed for monodisperse rings is still adequate to describe slightly polydisperse systems. This work appears to be one of the first observation of the Casassa form factor (eq 2) for macromolecules of ring topology.

By SANS Iwamoto et al. studied polystyrene (PS) ring melts over a wide range of molecular weight.[109] They determined the radii of gyration R_g of the ring polymers by the Guinier approximation. R_g was found to depend on the degree of polymerization N as $R_g \sim N^{\nu=0.47}$ that is in fact very close to linear chains with Gaussian statistics. The authors related the observation of such a large exponent ν to a contamination of the ring samples with linear chains. However, as will be shown below the contribution of linear chains to the ring form factor in the limit of highly concentrated rings in a linear matrix is relatively small.[110]

In our recent work we were able to identify the crossover from Gaussian chain statistics to a more compact conformation to occur at a distance along the ring corresponding approximately to the entanglement distance of the corresponding linear chain $N_{e,0}$.[21,56] At distances larger than $N_{e,0}$ along the ring contour length the compressed conformation is expected. This is clearly seen on the SANS data presented in the Figure 8. This finding was considered as a clear signature of the theoretically predicted elementary loops that build up the ring conformation.

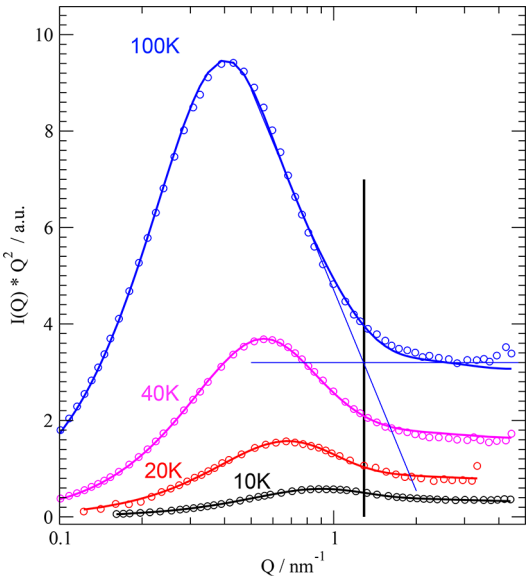

Figure 8. Kratky plot $I(Q)Q^2$ vs Q of the SANS data obtained for the rings of different sizes (10K: 10 kg/mol, 20K: 20 kg/mol, 40K: 40 kg/mol, 100 K: 100 kg/mol). For better visibility the data are shifted vertically by a factor of 2 with respect to each other. The vertical solid line marks the position of the crossover between the fractal and Gaussian regimes.

The compressed conformation is described in terms of the real space distances r between monomers i and j which relate to a monomer random walk more compact than Gaussian with a fractal dimension $d_f = \frac{1}{\nu}$:

$$\langle r^2\rangle \sim \left((|i-j|)\left(1-\frac{|i-j|}{N}\right)\right)^{2\nu} \quad (3)$$

with the exponent $\nu < \frac{1}{2}$. For mass fractals with a fractal dimension $d_f = 3$, $\nu = \frac{1}{d_f} = \frac{1}{3}$. The second term in eq 3 arises from the ring closure condition. The common exponentiation of both terms bases on an investigation by Bensafi et al.[111] For $|i-j| \leq N_{e,0}$ Gaussian statistics prevails and $\nu = \frac{1}{2}$ holds. We consider a smooth crossover between both regimes and describe it by a sum of Fermi functions of width ν_{width} centered at $N_{e,0}$. Then the ring form factor becomes

$$P(Q) = \frac{1}{N}\sum_{i,j}^{N}\exp\left[-\frac{Q^2l^2}{6}|i-j|^{2\nu_{eff}}\left(1-\frac{|i-j|}{N}\right)^{2\nu_{eff}}\right] \quad (4)$$

with

$$\nu_{eff} = \nu_{loc} + \left(\frac{\nu-\nu_{loc}}{1+\exp\left(\frac{N_{e,0}-|i-j|}{\nu_{width}}\right)}\right) \quad (5)$$

where $\nu_{loc} = \frac{1}{2}$ is the local chain expansion exponent and $\nu = 1/d_f$ the large-scale expansion exponent, l is a monomer length.

The solid lines in Figure 8 are the result of a joint fit of eqs 4 and 5 to the corrected SANS data. Thereby the length of the Gaussian substructures $N_{e,0}$ was varied jointly for all ring sizes,

https://doi.org/10.1021/acs.macromol.3c00560
Macromolecules 2023, 56, 7203−7229

while the other parameters: total intensity, fractal exponent ν and monomer length l were varied independently. In addition, to correct small mistakes in the background subtraction a flat background was considered that turned out to be in the order of 10^{-3}. With this approach a nearly perfect fit for all rings was achieved. For the crucial size of the Gaussian substructures taken as elementary loop size, we found $N_{e,0} = 45 \pm 2.5$. We note that this result contradicts the assertion of Sakaue, who proposed a topological mesh size that increase with N as $N^{1/5}$. For the investigated range of ring N a change of $N_{e,0}$ by a factor 1.5 would have been expected, which can be safely excluded.

Other than extracted from numerous simulations that are interpreted in terms of a crossover to mass fractal behavior with a fractal dimension $d_f = 3$ and $R_g \sim N^{1/3}$around $N \cong 10-15N_{e,0}$ such a crossover was not observed even for larger rings $N \cong 44N_{e,0}$. For the ring size, rather $R_g \sim N^{0.39}$ was found over the entire size range in good agreement with the results of Obukhov et al.[91] (eq 1).

Using neutron scattering we were able to scrutinize the result of Halverson et al. for large PEO rings up to $N/N_e \cong 44$.[56] As may be seen in Figure 6 without any correction factors the normalized simulation data follow very precisely the experimental results. As directly found by the measured N-dependence of R_g for the reduced chain length $N/3N_e$ values ($N_e = N_{e,0}$) the experimental points do not reach the asymptotic mass fractal regime and again other than insinuated by Figure 6 the crossover appears to be very broad.

3.2. Conformations of Ring-Linear Blends. One intriguing scientific challenge is posed by blends of ring and linear polymers. Blending rings with linear chains very strongly affects both, the ring conformation and dynamics. The ring conformations in a blend with linear chains at low ring concentration assume a Gaussian shape that is very similar to dilute rings in a θ-solvent.[112]

Because of specific topological interactions between rings and linear chains the ring conformation changes, and diffusivity is strongly reduced. Threading by linear chains leads to long-living correlations between the different topological specimens. As a consequence of topology, phase transition lines are shifted in the sense that blending of rings with linear chains increases the miscibility. Depending on concentration rings in a matrix of linear chains are swelling. The degree of swelling depends on the ring concentration, demonstrating a crossover from Gaussian conformation to the pure ring globule. Interestingly, at high ring concentration where the linear chains play a role of contaminant, the ring structure is not changed, in contrast to dynamics and rheological properties.

3.2.1. Theories and Simulations. Swelling of rings as a consequence of their topology was first addressed by Moore and Grosberg[113] by simulation. Theoretical investigations of ring-linear blends are limited to mean field and scaling theories. Scaling arguments based on the blob model was applied by Iyer et al., in order to describe the transition between swollen ring conformation at low ring concentrations and compact behavior for pure rings.[114] In the dilute region the sizes of the components are independent of the ring concentration or volume fraction ϕ_R. Above the ring overlap volume fraction the size of the linear component stays unchanged $R_{g,l} \sim (1 - \phi_R)^0$ and continues to be independent of the ring concentration. However, the ring size shrinks as $R_{g,r} \sim \phi_R^{-1/5}$ (Figure 9). The overlap concentration between the two regimes scales with $N_r^{-1/2}$ in agreement with the scaling for linear chains: for the larger rings the overlap concentration is smaller.

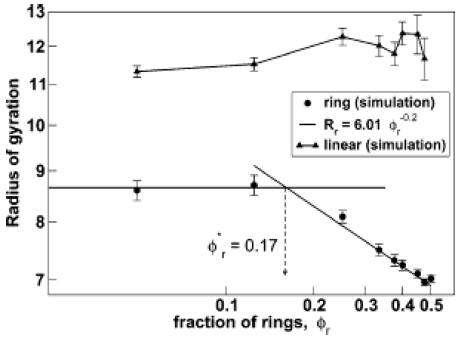

Figure 9. A log−log plot of the mean-squared radii of gyration of rings (circles) and linear chains (triangles) for a blend of ring and linear molecules with $N_r = N_l = 300$ at different compositions. The last six data points in the semidilute and concentrated region are used to fit the straight line to R_r.[114] Reproduced with permission from ref 114. Copyright 2007 American Chemical Society.

Using the bond fluctuation model (Monte Carlo simulations) Iyer et al. confirmed the main results of scaling approach.[114] Later the primitive path length and the average number of entanglements between rings and linear components (threadings) have been analyzed and were found to be independent of the blend composition.[115] In contrast, the primitive path length, and the average number of entanglements on a ring molecule increases approximately linearly with the fraction of linear chains, and for large N, they approached values comparable with linear chains.

By using polymers of different topology, i.e., rings and linear chains, the miscibility of polymer blends, a classical problem in polymer science, is altered. Sakaue et al. considered the idea of a topological free volume (TFV) as a basis for a mean field theory to clarify how the topological constraints in ring polymers affect the phase behavior of the blends.[116] While a large enhancement of miscibility is expected for ring-linear polymer blends, the opposite trend toward demixing, albeit comparatively weak, is predicted for ring−ring polymer blends. In the topological volume model of Sakaue the conformation of linear chains and rings up to the scale of $N_{e,0}$ is assumed to be Gaussian.[26] At larger scales, the rings get more compact and exhibit a tendency of mutual segregation. The conventional Flory−Huggins theory was adopted to represent the nontopological part of the free energy. To elucidate the topological effects, the condition under which Flory−Huggins-type approximations can be valid were determined. The authors clarify various length scales relevant to the polymer collapse and phase-separation in the ring-linear blend and determine the conditions for Gaussian conformation.

Atomistic MD simulation results of Jeong and Douglas obtained on polyethylene demonstrate significant swelling of the rings arising from altered self-excluded volume interactions.[99] A corresponding shape change is qualitatively similar to dissolving rings in a good solvent of small molecules. Calculating the gyration radii tensor, the shape of the rings in the linear matrix was found to be changed: going from more symmetric conformation at large ring concentrations to more elongated conformation at high concentration of linear chains.

On the basis of the atomistic MD of PEO Mavrantzas et al. concluded that the presence of linear chains (even in small amounts) can dramatically influence the underlying topological structure of the blend.[117] They pointed to strong and long-lived topological interactions—threadings—in the ring−linear blends which, however, leave the conformational properties of the linear

https://doi.org/10.1021/acs.macromol.3c00560
Macromolecules 2023, 56, 7203−7229

melt practically unaffected. Overall, threading of ring chains by linear molecules causes a dramatic reduction in the diffusivity and orientational relaxation of rings rendering the system's overall dynamics highly heterogeneous that is reviewed in detail in the chapter "Ring Dynamics".

The dependence of the ring size vs volume fraction of the ring ϕ_R in ring-linear blends $R_g \sim \phi_R^{-\alpha}$ was analyzed in work of Hagita et al. by coarse-grained MD simulations.[118] In particular, they investigated the ring-size dependence of the exponent α and ring−linear penetration for given ϕ_R analyzing the number of linear chain penetrations per ring (n_P). For the larger rings $\alpha = -0.09$ and for the smaller ones $\alpha = -0.06$ was obtained. Since α shows a dependence on the ring chain length, the results were used to compare R_g with the experimental data of Iwamoto et al.[119] At least for the larger rings the results agreed. On the basis of the analysis of n_P the author stated that the penetration of linear chains into the ring polymer is enhanced by a decrease of ϕ_R.

Very recently Grest et al. studied the entropic mixing of ring−linear polymer blends.[120] In the case identical monomers for both components they found a strongly negative Flory−Huggins parameter $\chi_{F,RL}$ that promotes ring-linear mixing. They also noted that the topological enthropy of mixing does not scale with the chain length $\chi_{F,RL} \sim -1/N$, but rather with the elementary loop length $\chi_{F,RL} \sim -1/N_{e,0}$ resulting in a very strong compatibilization effect.

3.2.2. Experiments. Using SANS, Kobayashi et al. studied conformation and miscibility of highly purified hydrogenous ring poly(4-trimethylsilylstyrene) (h-PT) and deuterated ring polyisoprene (d-PI) samples as well as their linear counterparts and their blends.[48] At 50/50 vol % concentration of the hydrogenated and deuterated components the authors find that in the low Q regime the scattering profiles of ring−ring blend exhibit much higher scattering intensity than linear−linear and ring−linear blends, while the latter two show similar profiles. On the basis of the miscibility analysis at a given temperature the concentration fluctuations are largest for the ring−ring blend and rather similar for the ring−linear and linear−linear blends. This indicates for the ring−ring blend a proximity of a phase transition which is not evident for the other two blends.

Recently we found that the ring radius of gyration R_g shrinks with increasing ring fraction and nearly reaches the R_g of the ring melt at a volume fraction of $\phi_R = 0.5$.[110] At the same time the fractal dimension d_f, which is close to a Gaussian conformation at low ϕ_R, increases to the value of the ring melt. Aside from very short matrices the ring size is independent from the host length. Following a random phase approximation (RPA) treatment, the effective Flory−Huggins parameter ($\chi_{F,RL}$) is negative and independent of ϕ_R, signifying ring-linear attraction that leads to ring−ring repulsion. $\chi_{F,RL}$ decreases with decreasing ring size, which might relate to the decreasing possibility of threading events, when the ring size becomes smaller. The ϕ_R dependent data at low Q before the Porod scattering Q^{-4} regime display a Q^{-2} intensity regime, the intensity of which increases proportional with ϕ_R. The origin of this Q^{-2} contribution is not clear but may relate to critical fluctuations or microphase separation induced by a nonlocal positive contribution to $\chi_{F,RL}$. The experimental results fit well into the general picture that mainly bases on simulations, even though in detail quantitative differences are obvious. Finally, these results are in qualitative agreement with earlier studies on PS ring-linear blends.

3.3. Perspectives: Ring Conformations. It has been stated experimentally and confirmed by simulations that the conformation of ring macromolecules in the pure ring melt is more compact than that of linear counterparts. This is a consequence of the topological constraints acting on nonconcatenated rings leading to conformational self-similarity on scales beyond the elementary loop size. The ring polymer is built by elementary loops−characterized by Gaussian statistics, as stated by theories, and supported by simulations and scattering experiments on different synthetic polymers. However, the larger scale effect of double-folded conformations described by theories has never been observed experimentally. Some simulation works report the "double-folded" conformations of the ring polymers.[76] The others do not find an indication of the tree-like structures.[15,117] In the respective calculation of Halverson et al. the directional distribution of vectors along the chain was investigated reaching out to different spatial volumes.[15] For all distances up to a distance $2\langle R_g^2(N_{e,0})\rangle^{1/2}$ the vectors assumed random orientations confirming that rings in the melt are not double stranded. Such a finding casts severe doubt on approaches which are based on lattice animal arguments. As mentioned in ref 121, double-folded conformations of rings in the melt are rather questionable and may be an artifact of very long relaxation times of such structures. In light of these results, the question needs to be posed, whether the tree structures found in simulations relate to the initial double folded structures that are imposed as the starting conformations. One may have to rethink, how to construct "by first-principles" equilibrated solutions of ring polymers not based on double-folded conformations. Experimental works on the ring conformation should focus on an analysis the data in terms of tree-like "double-folded" structures.

Another interesting direction is related to the topological glass state in ring melts and their blends found by theory and simulations. The role of the mixing entropy as a function of a ring loop size and ring dimension is another aspect of the physical properties of ring-linear blends.

In general, theoretical investigations mainly focus on the description of flexible ring polymers that may not be correct for the locally stiff DNA-like polymers or some synthetic polymers with certain segmental stiffness.[122,123] Deviations from the Gaussian conformational statistics on the chain or subchain level would result in additional topological constraints. The question of local chain stiffness was considered by Sakaue.[93] He predicted that the crossover to compact statistics $R \sim N^{1/3}$ (fractal behavior) decreases sharply with increasing stiffness, meaning that the topological effects are even more important for worm-like ring chains such as DNA. Coarse-grained simulations of Stano et al. demonstrate lower mixing energies for rings with increasing bending stiffness, in contrast to their linear counterparts, which are known to demix into two phases.[124] Flexible and stiff rings demonstrate quite different threading behavior: Flexible rings pierce the surface of the other ring several times but only shallowly, as compared to the stiff rings which pierce less frequently but deeply. This demonstrates the conditions for the threading mechanisms essentially change with the ring stiffness. Systematic experimental investigations of the increased ring stiffness on the conformational properties accompanied by topological phase investigation are missing. They could transfer the problem in the direction of biology.

4. RING DYNAMICS

4.1. Theory and Simulations. Early works considered the conformation and motion of polymer rings through an array of fixed obstacles. The DFLA model[92] proposed an analogy to randomly branched polymers—the lattice tree model, where

https://doi.org/10.1021/acs.macromol.3c00560
Macromolecules 2023, 56, 7203−7229

relaxation occurs by the retraction of double folded strands leading to a terminal relaxation time $\tau_d \sim N^3$ with N being the number of monomers, fractal dimension of $d_f = 4$ and a COM diffusion $D \sim N^{-2}$. Later, the model was refined correcting the terminal time to $\tau_d \sim N^{2.5}$. In this work Grosberg dismissed the unrealistic limiting fractal dimension of the DFLA model and considered a skeleton lattice tree that branches randomly at an entanglement spacing $d_{tube} = lN_{e,0}^{1/2}$, resulting in a fractal dimension of the backbone or trunk of the lattice tree of $d_b = 5/3$, the statistics of a self-avoiding random walk.[125]

For the dynamics of this self-similar structure, Grosberg derived $\tau_d \approx \tau_e(N/N_{e,0})^{2.56}$, where τ_e is the entanglement time.[18]

The self-consistent FLG model conjecturing that the overlap of loops is limited by an overlap criterion, similar to that for linear melts, also leads to a limiting fractal dimension of $d_f = 3$.[95] As the FLG model has been thoroughly studied experimentally, we discuss this model in some detail. An important observation in establishing this model was that in a melt of rings, the topological constraints are diluting with the progressing time, because with time loops of increasing sizes are relaxed and cease to be obstacles in a similar way as tube dilation occurs, e.g., in polydisperse linear melts.[4,126,127] The time scale is set by the time a loop of a given size has traveled over its own size defining, thereby, the effective time-dependent tube diameter

$$d(g, t) = \langle r_e^2(g)\rangle^{1/2} = \langle \Delta r_{com}^2(g, t)\rangle^{1/2} \tag{6}$$

where r_e is the diameter of a loop containing g monomers and Δr_{com}^2 is the mean squared displacement of the loop COM. The equation holds for complete tube dilation, which is supported by MD-simulations.[98] For $d_f = 3$, the time-dependent tube diameter becomes $d(g,t) \cong d_0[g(t)/N_{e,0}]^{1/3}$ and $d(N_{e,0}, \tau_e) = d_0$. The FLG model, assuming complete tube dilation, is also termed self-consistent FLG model and leads to

$$\tau_d = \tau_e\left(\frac{N}{N_{e,0}}\right)^{2+1/d_f} \tag{7}$$

For the COM diffusion constant the model predicts

$$D_{com} \cong \frac{R_g^2}{\tau_d} \; D_{R,e}\left[\frac{N}{N_{e,0}}\right]^{-2+1/d_f} \tag{8}$$

with $D_{R,e} = d_{tube}^2/\tau_e$ being the Rouse diffusion coefficient of one elementary loop. Without tube dilation in the naïve FLG model, the terminal time is $\tau_d \cong \tau_e\left[\frac{N}{N_{e,0}}\right]^{2+d_b/d_f}$ and the COM diffusion becomes $D_{com} \cong \left[\frac{N}{N_{e,0}}\right]^{-2+(2-d_b)/d_f}$. Self-similar relaxation implies that any section of the ring larger than $N_{e,0}$ relaxes in the same way as the whole ring; thus, the FLG model for a mode "p" leads to

$$\tau_p = \tau_e\left(\frac{N}{pN_{e,0}}\right)^{2+1/d_f} \tag{9}$$

and correspondingly, for the naïve FLG model $\tau_d \cong \tau_e\left[\frac{N}{pN_{e,0}}\right]^{2+d_b/d_f}$. Given this property, we call the scaling models also spectral models and the exponents spectral exponents. On the basis of the experimentally determined fractal ring dimensions of the PEO rings $d_f = 1/\nu$[21] with small variations owed to slightly different ν, for the spectral exponents, the models predict: FLG: 2.45; DFLA: 2.5; Grosberg: 2.75; naïve FLG: 2.9.

Aside from theoretical modeling, a significant number of MD simulations is available. Using coarse grained models, the largest MD simulation effort so far is due to Halverson et al., where rings up to $57N_{e,0}$ were simulated.[128] In disagreement to the predictions of the scaling models, for ring COM diffusion, they found $D_{com} \sim N^{-2.3}$. Furthermore, the N-dependencies of the ring and linear counterparts were found equal, with the prefactor for ring diffusion about seven times larger than that for linear chains. In agreement with theoretical predictions, for early diffusion, the simulation revealed subdiffusive behavior $\langle r_{com}^2(t)\rangle \sim t^{0.75}$ up to times and distances of about two to three times R_g. The internal rearrangements of longer rings were found to occur much faster than the time it takes to diffuse over their own size. But, alternatively, the $t^{1/4}$ regime in the segment self-correlation function extends to two to three times of R_g; there exists no second $t^{1/2}$ regime as for linear chains.[1] The rings were found to relax stress much faster than linear polymers, and the zero-shear viscosity was observed to vary as $\eta_0 \sim N^{2.2\pm0.3}$ which is weaker than the $N^{3.4}$ behavior of linear chains, but stronger than that of commonly known models for polymer dynamics.[129]

Atomistic simulations on large PEO rings on 10 kg/mol and 20 kg/mol samples were analyzed in terms of Rouse modes that were found to provide an orthogonal basis also for rings.[130] The analysis in terms of Rouse modes revealed that the power law exponent for the Rouse spectrum $\tau_p \sim p^2$ did not change even for the largest ring, while the Rouse amplitudes were diminishing for low p. Very recently, Wong and Choi in terms of a united atom model presented MD-simulation for PE rings in connection with the PRISM theory, where aside from normal Fickian diffusion, a short time regime with $\langle r_{com}^2(t)\rangle \sim t^{0.42}$ was observed.[131]

Finally, Michieletto and Sakaue reported a "dynamical entanglement analysis" (DEA) with the aim to extract spatial and temporal entanglement structures from the pairwise displacement correlation of the entangled chains. Applying this method to large-scale molecular dynamics simulations of linear and unknotted, nonconcatenated ring polymers, they found strong cooperative dynamics.[132]

4.2. Threading Phenomena. Rings tend to interpenetrate each other, a mechanism called threading. Such threadings are believed to strongly affect the dynamics, as their relaxation might become much slower than the longest ring internal relaxation. One important manifestation of this phenomenon is observed for the dynamic modulus of ring melts. The self-similar models predict a power relaxation[133] as

$$G(t) = \left(\frac{t}{\tau_0}\right)^{-2/5} \exp\left(-\frac{t}{\tau_d}\right) t > t_e \tag{10}$$

where τ_d is the longest internal relaxation time. Figure 10 displays results from polyisoprene (PI) and PS ring melts.

Even though there is a very good agreement between theoretical predictions, simulations and experimental results in the power law regime, severe deviations are present at longer times. Clearly the single exponential decay predicted by theory is not present—the relaxation processes extend to much longer times. Such long-time relaxation processes might be related to small amounts of linear contaminants and/or ring−ring threading.

In order to clarify the role of threadings, Tsalikis et al. have performed a geometrical analysis of atomistic simulation data of

https://doi.org/10.1021/acs.macromol.3c00560
Macromolecules 2023, 56, 7203−7229

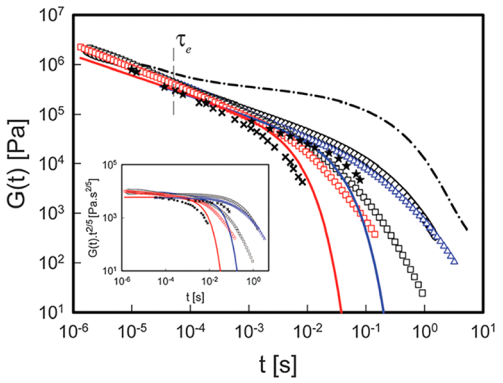

Figure 10. Stress relaxation modulus for PI and PS rings at $T - T_g = 65$ °C:PI 81 kg/mol (blue triangle); PI 38 kg/mol (red square); PS 198 kg/mol (black diamond); PS 160 kg/mol (black square). The stars and the crosses are from molecular dynamic simulations on coarse-grained bead−spring rings with $Z \approx 3.6$ and 14.4. The blue and the red lines are model predictions for PI 81 kg/mol and 38 kg/mol, respectively. The dash-dotted line is the relaxation modulus for the PI 81 kg/mol linear polymer, exhibiting an entanglement plateau. The Rouse time for entanglements, τ_e, of the linear PI 81 kg/mol is also depicted for reference. Inset: Scaled version of the same plot, without the linear polymer data for clarity.[129] Reproduced with permission from ref 129. Copyright 2013 American Chemical Society.

monodisperse PEO rings.[23] The analysis involved three steps: (1) The ensembles were reduced to coarse-grained paths; then (2) the resulting three-dimensional polygons were triangulated; and finally, (3) the interpenetrations were identified by vector calculus, thereby, locating ring−ring threading events and quantifying their strength and survival times. Figure 11 displays such a threading event identified for the 10 kg/mol PEO melt.

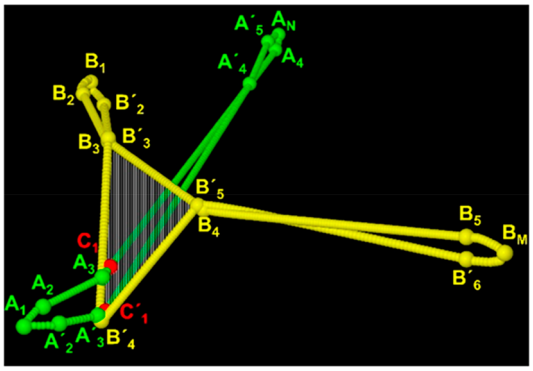

Figure 11. Snapshot from the geometric analysis of the 10 kg/mol PEO melt, demonstrating the threading of a ring PEO molecule (represented by the sequence of yellow beads and strands) by another ring molecule (represented by the sequence of green beads and strands), after the reduction of the corresponding atomistic chains to primitive paths.[23] Reproduced with permission from ref 23. Copyright 2016 American Chemical Society.

The simulations reveal single and multiple threading events, which appear to dominate at least for the largest ring. The amount of multiple threadings was found to increase linearly with ring size. For the larger rings the lifetime of these threadings were observed to extend up to several times the longest ring internal relaxation time.

Smrek et al. investigated the effect of threading phenomena in the context of the randomly branching tree model that bases on double folded structures. This model describes unconcatenated ring polymers in concentrated solutions and melt remarkably well. However, the tree model does not comprise the significant interpenetration of adjacent rings in the form of long-lived topological constraints or threadings. In order to better understand the occurrence of such threadings the authors employed a minimal surface concept.[24] As illustrated in Figure 12, in this model rings are considered as threaded if their minimal surface is crossed by another ring.

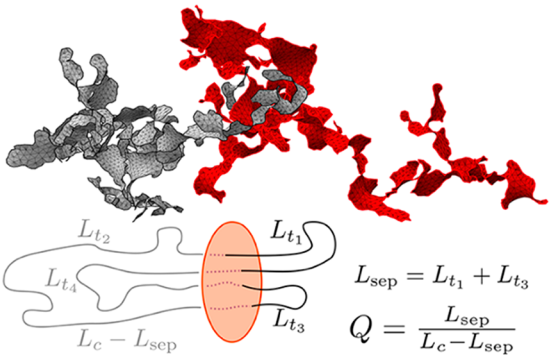

Figure 12. Top: Minimal surfaces of a pair of close-by rings modeled as double-folded polymers on interacting branched primitive trees (IBP model). Bottom: Schematic representation of one ring (black and gray) penetrating the minimal surface of another ring (orange) of total contour length L_c and L_{t_i} is the contour length of subchain i penetrating the second ring. In this example, four surface penetrations split the penetrating ring into the segment pairs (L_{t_1}, L_{t_3}) and (L_{t_2}, L_{t_4}) which are on opposite sides of the surface this defines the separation length, L_{sep}, and its complementary, $L_c - L_{sep}$.[24] Reproduced with permission from ref 24. Copyright 2019 American Chemical Society.

The authors show that tree models are incomplete as they underestimate the amount of threading. The relaxation of threadings take the form of a power law and the connected time scales match those of COM diffusion and are substantially longer than the internal relaxation.

Also Ubertini et al.[96] investigated the apparent contradiction between the view of rings as double folded structures in the melt state and the phenomenon of ring threading. While simulations appear to support the tree picture on a single ring level, in particular dynamic studies show that rings thread each other, a feature not present in the tree theories. Using Monte Carlo simulations of ring melts with different bending rigidities the simulations show that rings are double-folded on the scale of the entanglement length $N_{e,0}$, while the threadings are localized on smaller scales. However, as discussed in the section 3.3, double-folded structures appear not to exist in ring melts.

4.3. Experimental Observations on the Scale of the Ring−Neutron Scattering. As a result of the difficulties to synthesize well-defined large ring polymers with fast enough local dynamics to be observed by quasi-elastic neutron scattering techniques (QENS), only recently reports are found in the literature. These techniques are limited to relaxation times faster than 500 to 1000 ns (Neutron Spin Echo, NSE). First NSE experiments were reported by Bras et al.,[134] who compared the dynamics of a M_w = 2 kg/mol PEO ring with its linear counterpart. The COM diffusion as compared to the linear polymer was found to be significantly faster than expected. While the smaller R_g and the lower viscosity of the rings are in quantitative agreement with the Rouse theory, the much faster

https://doi.org/10.1021/acs.macromol.3c00560
Macromolecules 2023, 56, 7203−7229

diffusion demonstrates an obvious violation of this model. The COM diffusion is clearly not solely determined by segmental friction and the number of segments as predicted in the Rouse model. In contrary it shows an unexpected dependency on the architecture.

In 2014 the same group studied the dynamics of PEO rings of a molecular weight amounting to 2.5 N_e = 5 kg/mol.[135] Among others in a surprising analogy to the cage effect known from glassy dynamics, the NSE experiments revealed pronounced non-Gaussian (NG) behavior of the COM diffusion. Correcting for the Gaussian approximation for $S(Q, t)$ to first order NG effects are described in terms of a fourth order contribution in Q:

$$S(Q, t) = \exp\left[-\frac{\langle r^2(t)\rangle Q^2}{6} + \frac{\alpha(t) Q^4 \langle r^2(t)\rangle^2}{72}\right] \quad (11)$$

with $\alpha(t)$ the NG-parameter. Figure 13 displays $\alpha(t)$, as obtained from the experimental data. Comparing with results from molecular glass formers the shape of $\alpha(t)$ is a typical result of a cage effect.

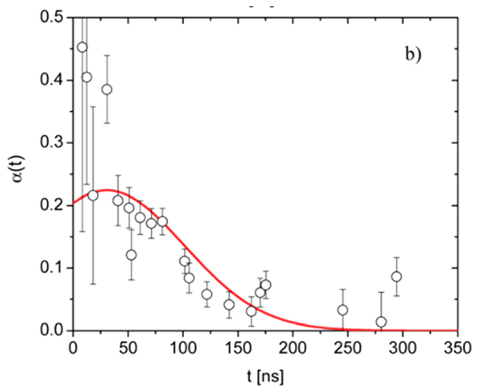

Figure 13. Non-Gaussian parameter $\alpha(t)$ as obtained from the NSE spectra due to COM motion. The points result from a point-by-point analysis of the spectra at different Q; the solid line is obtained from a fit of the data with eq 11.[135] Reproduced with permission from ref 135. Copyright 2014 The Royal Society of Chemistry.

With the increasing capabilities of ring polymer synthesis, recently very large rings in terms of $N/N_{e,0} < 45$ became available allowing at test of the different scaling models for the self-similar ring dynamics.[21,30,56,135,136] Altogether the dynamics of 4 different well characterized PEO ring melts with $5 \leq N/N_{e,0} \leq 44$ were studied. Figure 14a presents the COM MSD for the 2 smallest rings (10 kg/mol ≡ $R10$ and 20 kg/mol ≡ $R20$); they were derived from the dynamic structure factor as $\langle r^2_{com}(t)\rangle = -\frac{6}{Q^2}\ln[S(Q, t)]$. Figure 14b demonstrates the molecular weight dependence of the ring Fickian diffusion coefficient.

Figure 14a displays the 3 dynamic regimes for the COM diffusion: at early times the COM MSD is strongly subdiffusive with an exponent that decreases with increasing ring size. At $\langle r_1^2\rangle$ it crosses over to the theoretically predicted $t^{0.75}$ regime. Finally, at $\langle r_2^2\rangle$ the Fickian regime is approached. For R10, where the second crossover could be observed directly, we have $\langle r_1^2\rangle/R_g^2 \cong$ 2.6 in very good agreement with Halverson's simulation. From the ratio of the values for $\langle r_1^2\rangle$, which was found to be very close to the ratio of the respective radii of gyration, it was concluded that the first crossover might relate to cooperative dynamics resulting from the correlation hole as predicted by Guenza for linear polymers.[137] From Figure 14b we observe that the Fickian diffusion coefficients as a function of ring size follow a very similar power law as that for their linear counterparts in good agreement with simulation and the topological free volume theory of Sakaue. However, the result disagrees with the predictions from the scaling models that always predict power law exponents less than 2 (see eq 8)

At scales below the elementary loop size the internal dynamics is well described by ring Rouse motion. As may be seen from Figure 15 at larger scales the dynamics is self-similar and follows very well the predictions of the scaling models with preference for the FLG model.

We note that over the full time regime up to the longest times the spectra perfectly agree with the scaling model with no sign of any retardation that might be related to threading events.

The segmental MSD may be directly studied by incoherent neutron scattering, which measures the self-correlation function of the protons. In this case, the structure factor arising from the self-correlation function has the form:

$$S(Q, t)_{self} = A(Q)\exp\left[-\frac{Q^2}{6}\langle r^2(t)\rangle\right] \quad (12)$$

where $\langle r^2(t)\rangle$ is the average MSD of a monomer containing both motion by intra chain relaxation as well by translational COM diffusion and $A(Q)$ is the Debye−Waller factor. Figure 16 displays the $\langle r^2(t)\rangle$ for the 100 kg/mol ring ($R100$) and its linear counterpart L100, that following eq 12 were evaluated from the incoherent spectra.

As predicted by the Rouse model, initially the MSD follows a $t^{1/2}$ power law. Then, for the linear chain at a crossover time $\tau^{self} \cong 8$ ns, the power law weakens and changes to a time dependence compatible with $t^{1/4}$ power law, which is expected for local reptation. While for the linear chain the crossover to local reptation is evident, for the ring, the relative slowing down of the MSD appears to be somewhat less pronounced and takes place at a later time (13.5 ns). Finally, Figure 17 displays the results for the $R100$ ring in the context of the overall picture of ring dynamics, as it was derived on the basis of the coherent scattering explained above. Using the model parameters obtained from the spectral fit, the predictions for the MSD due to translational and internal motion are estimated up to times in the order of 10^6 ns, where Fickian diffusion takes over. The red dashed-dotted line presents the segmental MSD, while the green solid line marks the COM MSD. Both add to the solid blue line describing the total MSD of a segment that is observed by the incoherent experiment. It is very satisfying to find the excellent agreement between the data for the self-correlation function obtained in an independent experiment with the prediction based on the coherent scattering data underlining the consistency of the data evaluation.

Finally, measuring the self-correlation function by incoherent scattering, the dynamics on the segmental level for PDMS rings was investigated by Arrighi et al.[138] For linear PDMS see also.[139] Having available only small rings of a size up to about $2N_{e,0}$, the focus was on the effect of ring closure on the segmental dynamics by a comparison with linear counter parts. First of all, the results show, that the rather prominent CH_3 group rotation is not affected by the ring topology. For the smaller rings the data reveal that the segmental relaxation times for rings are always longer than those of the corresponding linear polymers. Partly this relates to the presence of chain ends that are not existing for rings. However, as the authors show, for small rings missing chain

https://doi.org/10.1021/acs.macromol.3c00560
Macromolecules 2023, 56, 7203−7229

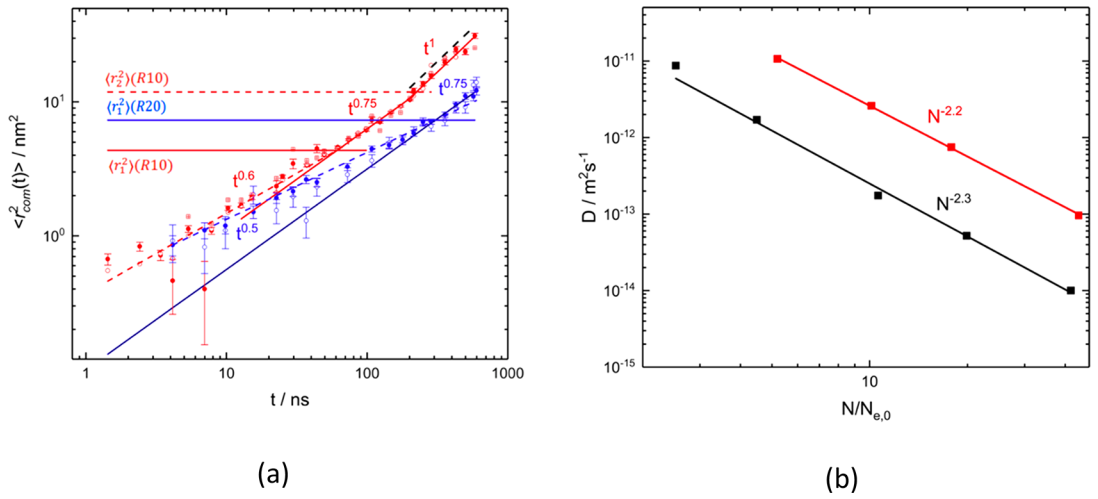

Figure 14. (a) COM MSD as evaluated directly from the measured dynamic structure factors for 10 kg/mol (R10, upper red) and 20 kg/mol (R20, bottom blue). Red crossed squares, open and filled circles correspond to $Q = 0.3$, 0.5, and 0.8 nm^{-1} for R10; blue filled and open circles relate to $Q = 0.3$, 0.5 nm^{-1} for R20. The horizontal lines mark the different crossovers $\langle r_1^2 \rangle$ and $\langle r_2^2 \rangle$. Dashed black line shows the MSD extrapolated from the PFG-NMR diffusivity measured for R10 ring. (b) PFG-NMR results for the diffusion constants of rings in the melt (upper red squares) as a function of chain length. Bottom black squares show diffusion coefficients for corresponding linear PEO melts.[56] Reproduced with permission from ref 56. Copyright 2021 AIP Publishing.

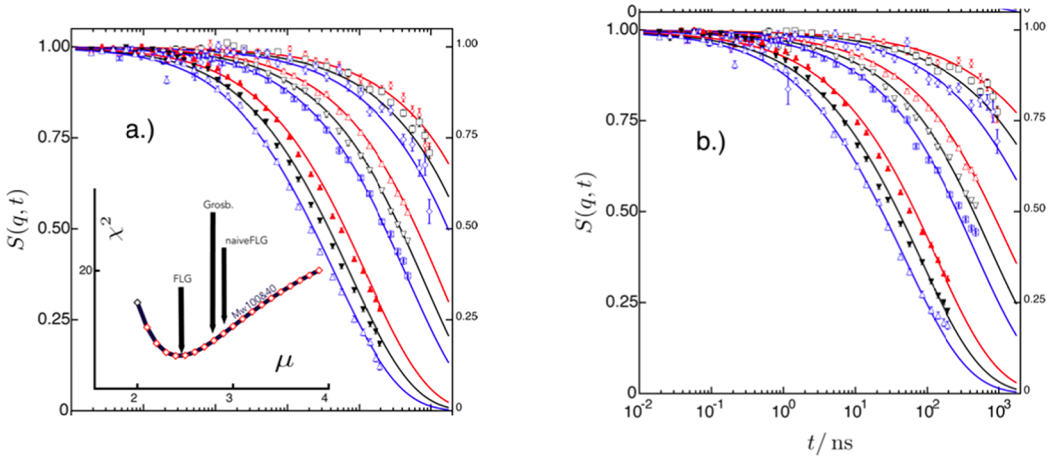

Figure 15. NSE-spectra addressing the intra ring pair correlation function (a) from the 40 kg/mol ≡ *R*40 melt and (b) from 100 kg/mol ≡ *R*100 melt; the *Q*-values from above are 0.42, 0.49, 0.55, 0.69, 0.78, 0.86, 1.1, 1.2, 1.3 nm^{-1}. The solid lines present the best joint fit using the self-similar scaling model. The inset displays the mean squared error χ^2 from the combined fit of the R40 and R100 rings as a function of the spectral exponent μ. The errors indicate the expectations from the different scaling models.[22] Reproduced with permission from ref 22. Copyright 2020 American Physical Society.

ends alone cannot explain the rather important slow-down of relaxation. As the local relaxation takes place through rotational transitions around the main chain bonds, apparently ring closure for small rings imposes constraints for these transitions. With increasing molecular weight the relaxation times of rings and linear polymers approach each other—the constraints cease to exist.

4.4. Challenges for the Future: Pure Ring Dynamics.

We have presented self-similar scaling approaches that are proposed to capture the dynamics of ring melts. These models were refined several times to culminate in the self-consistent FLG model of Rubinstein. These models were thoroughly investigated by NSE that covers the proper time and length scales. The data analysis showed that the data are in best agreement with the FLG model. The study of the rheology of large rings displayed a power law regime as predicted by the scaling theories. However, the longtime cut off of $G(t)$ was found to be much broader than expected from self-similar dynamics. These finding triggered simulations searching for long living inter ring threadings, which were evidenced in large atomistic MD simulations. Similarly, the translational diffusion exhibits a much stronger dependence on molecular size than predicted by scaling models. Finally, also the double-folded conformations displayed by simulations are not established yet. With this state of the art a number of open questions need to be solved in the future:

- In view of contradicting simulation results, double-folded conformations of rings in the melt are rather questionable and may be an artifact of very long relaxation times of such structures. Considering these results, the question needs to be posed, whether the tree structures found in simulations relate to the initial double folded structures that are imposed as the starting conformations. One may have to rethink how to construct "by first-principles" equilibrated solutions of ring polymers not based on double-folded conformations.[121]

https://doi.org/10.1021/acs.macromol.3c00560
Macromolecules 2023, 56, 7203−7229

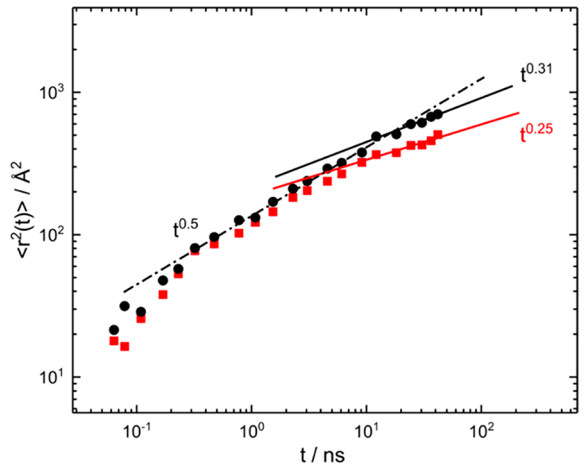

Figure 16. Segmental MSD derived from the incoherent spectra from the R100 ring. The lines present the limiting power laws for Rouse motion ($t^{1/2}$) and local reptation ($t^{1/4}$) and an empirical power law for rings.[56] Reproduced with permission from ref 56. Copyright 2021 AIP Publishing.

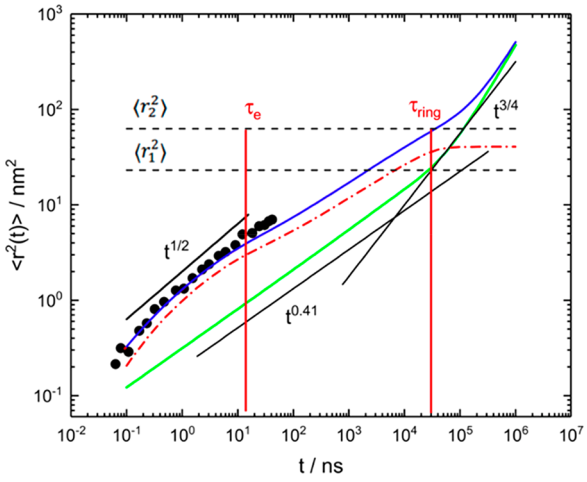

Figure 17. Comparison of the segmental MSD for the R100 ring, directly obtained from the self-correlation function (incoherent scattering) (symbols). The solid blue line presents MSD calculated from the best fit of the pair correlation function. Dashed horizontal lines show the $\langle r_1^2 \rangle$ and $\langle r_2^2 \rangle$. The solid green line represents the COM MSD and the red dashed-dotted line is the segmental MSD. The black solid lines demonstrate power laws as indicated in the figure, the vertical lines τ_e, $\tau_{ring} = \tau_d$ indicate the loop Rouse time or entanglement time and longest relaxation time of the ring, respectively. The figure extends the time range showing the predicted full dynamic regime based on the obtained fit parameters.[22] Reproduced with permission from ref 22. Copyright 2020 American Physical Society.

- The degree of cooperativity of motion is another very interesting issue: Using a novel dynamical entanglement analysis (DEA) Michieletto and Sakaue opened the way to quantitatively study dynamic correlations between pairs of polymers albeit rings on the level of diffusion.[132] In the future it would be interesting to study such cooperativity on the monomer or even better on the level of entanglement strands. The observed long and spatially extended cooperativity using DEA and the notion of entrainment may explain the discrepancies of rheology experiments with theories for linear[129] and ring[17] polymers and their long subdiffusive regime compared with their self-diffusion time. The experimentally observed 3 diffusive regimes with strong subdiffusivity at early times was tentatively related to a correlation hole effect, a deeper theoretical foundation is still missing.[22]
- The molecular weight dependence of ring melt viscosity $\eta \sim N^{2.2\pm0.3}$ identified in recent experiments is stronger[129] than both molecular dynamics simulation results[128] and various scaling model predictions. This discrepancy is likely due to minute contaminants of linear polymers in a ring melt, which enhance the melt viscosity with respect to that of pure rings. More systematic purification and characterization of ring polymers are needed to investigate the long time "foot" in the stress relaxation function and to obtain a more accurate estimate of the molecular weight dependence of pure ring melt viscosity.
- NG dynamics has been identified experimentally for rings with $N/N_{e,0} = 1$ and $N/N_{e,0} = 2.5$ that show a time dependent NG-parameter related to a cage effect well-known for glass forming liquids. For the small ring with an M_w corresponding to the elementary loop size, the decaging time determined at the peak position α_{max} of $\alpha(t)$ directly relates to the decorrelation time for COM diffusion. For the larger ring the decaging time (30 ns) was found to be a factor of 4 shorter than the diffusion decorrelation time (125 ns). With the first $p = 2$ internal mode suppressed, the first active mode $p = 4$ also is a factor of 4 faster than the nonactive first mode. Could it be that the caging relates to the elementary loop size and not to the full molecule?
- Finally on the segment level for small PDMS rings a retardation of the segmental relaxation time compared to the linear counterpart was observed. Beyond the correction for free ends, this essential intramolecular process seems to be affected by the closure constraint in ring molecules which slows down the segmental relaxation. The smaller the ring, the more pronounced is this effect. It remains to be seen, whether this is a feature of the PDMS samples is applicable to other ring systems such as PEO rings.

4.5. Ring−Linear Blends. Blends of ring and linear polymers pose fascinating challenges. While in such blends the dynamics of linear chains is hardly affected, minute concentrations of linear chains have a large effect on ring rheology.[17] Early investigations on the dynamics of ring linear blends focused on the diffusion of the constituents. Very instructive experimental results were reported by the Kramers group[140] on blends of dilute PS rings in linear matrices. The authors observed a strong slowing down of ring diffusion with increasing host molecular weight as well as for increasing ring size in identical matrices. The experimental results were discussed in terms of three basic diffusion mechanisms: (i) small rings are not confined by entanglements and perform Rouse type diffusion; (ii) among the rings threaded by host molecules, once threaded species are thought to move following the contour of the long linear chain; and (iii) finally multiple threaded rings diffuse by constraint release by the linear host.

Also, early rheological results were reported in the late eighties and nineties of the last century.[141,142] Larger efforts started in the late 2000s. In 2008 Subramanian and Shanbhag used a lattice model to estimate the self-diffusivity of entangled ring-linear blend in various compositions.[115] To interpret simulation results, they proposed a constraint release (CR) model for the

https://doi.org/10.1021/acs.macromol.3c00560
Macromolecules 2023, 56, 7203−7229

diffusion of a ring polymer threaded by linear chains, which propounds that CR processes enacted by the linear component progress in series. In a large scale simulation Halverson et al. investigated the structure, dynamics and rheology of ring-linear blends up to 14 entanglements.[16] In qualitative agreement with Kapnistos et al.[17] they found that small amounts of linear chains in a ring melt affect the ring melt viscosity at a concentration well below their overlap concentration. Ring diffusion is found to decrease with increasing fraction of linear chains. Above about the overlap concentration of linear chains ring diffusivity is strongly reduced. A 50/50 blend ring diffusion was observed to be slowed down by a factor of about 75 compared to the pure ring melt. However, the linear chains are hardly affected.

By PFG-NMR Kruteva et al. investigated the diffusion of differently sized PEO rings in linear PEO matrices of various molecular weights that revealed the astonishing result of two distinctly different diffusion modes for larger rings in entangled linear hosts: (i) fast diffusion that depends inversely on the host chain length and (ii) much slower diffusion depending much more strongly on the host molecular weight.[29] In contrast, the diffusion coefficient for a ring with a M_w corresponding to the entanglement length N_e in entangled hosts does not depend on the host size. Figure 18 displays an overview of the observed diffusion coefficients for rings of different M_w as a function of the host size.

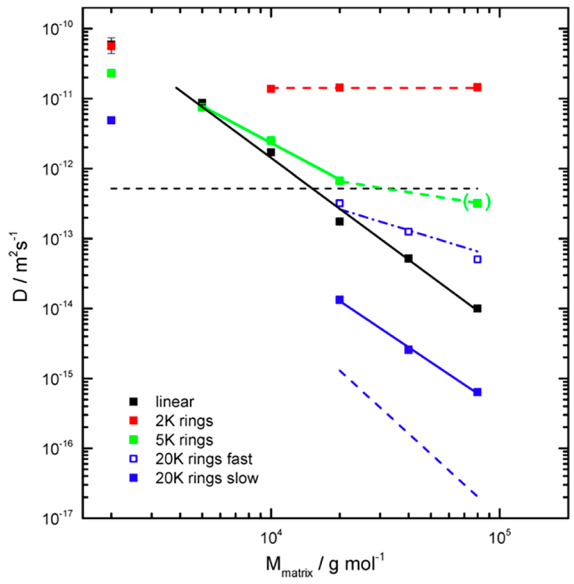

Figure 18. COM diffusion coefficients of different rings as a function of molecular weight of the host: dashed red line, matrix independent diffusion of the 2 kg/mol ring; full black line, power law behavior of linear chain diffusion $D_{COM} \sim N^{-2.4}$; solid blue line, slow diffusion mode for the 20 kg/mol ring, dashed black line, prediction for the reptation diffusion of a flat 20 kg/mol ring in the tube provided by the matrix; dashed-dotted blue line, prediction for diffusion of a once threaded 20 kg/mol ring; dashed blue line, prediction for diffusion by constraint release of a 20 kg/mol ring.[29] Reproduced with permission from ref 29. Copyright 2017 American Chemical Society.

The observations of two well-separated diffusion modes contradict simulation results that all find a broad distribution of heterogeneities compatible with a CR picture with no further evidence of a fast mode.[28,117,143] The observed two-mode structure supports the hypothesis of qualitatively different possibilities for the rings to diffuse. Quantifying the scaling predictions, the authors find that the fast mode quantitatively agrees with the assertion of a diffusion mode for once threaded rings[140]

$$D_{R1} \cong \frac{8}{15} D_0 \frac{N_e}{N_R N_L} \tag{13}$$

with $D_0 = \frac{k_B T}{\xi}$ where ξ denotes the monomeric friction. The suggestion of unthreaded rings undergoing reptation in the tubes provided by the host could not be supported. For the slow mode, different predictions are presented in the literature. From Figure 18 it is evident that diffusion by a conventional CR process $D_{CR} \cong \frac{4}{15} D_0 \frac{N_e^3}{N_R N_L^3}$ would be too slow (dashed blue line). However, following Klein's suggestion of a mutual dependency of constraints[144]

$$D_R = \frac{N_e^2}{2 N_R N_L^{1/2}} D_{rep}(N_L) \tag{14}$$

without any adjustable parameter the slow mode was shown to nearly quantitative agree with this approach. In eq 14 D_{rep} denotes the reptation diffusion coefficient of the linear host, which was measured independently. We note that with this approach also the M_w-dependence of the matrix diffusion may be described naturally. Finally, the two well-defined significantly different diffusive modes with characteristic times in the millisecond range would be expected to interchange. However, a detailed analysis in terms of a two-state diffusion model allowing for state changes clearly shows that within the experimental sensitivity of several seconds no such exchanges take place.[145,146]

Scrutinizing Kruteva's observations by atomistic MD-simulations Tsalikis and Mavrantzas showed that ring diffusivity is governed by the rate with which threadings are created and released and hypothesized that ring−linear threadings are the key mechanism governing dynamic behavior of ring−linear polymer blends.[147] These threadings, which in most cases are multiple threadings, cause rings to swell considerably and to move slower compared to their own melt. Concerning the diffusion of rings in short linear host or the diffusion of small rings in long entangled hosts the MD-results are in qualitative and quantitative agreement with the PFG-NMR data. However, the simulations do not reproduce the observation of two well separated diffusive modes for large rings in strongly entangled linear melts. Finally, we note that presently no good theoretical explanation for the fast diffusion exists. Further studies on different polymer systems would be desirable.

Also, in a very recent dynamic Monte Carlo (MC) study using the bond fluctuation model[148] the authors investigated the diffusion of differently sized rings in a linear host of different length.[149] As the NMR and the MD simulations above for small rings the diffusion coefficient was found to be independent of the linear host length. For large rings the authors found a self-diffusion scaling with an exponent between −1 and −1.5, indicating a scaling behavior similar to the intermediate 5K ring in the NMR study (see green line in Figure 18). The case of large rings in long linear melts apparently was not touched.

Similar to the study on ring melts, Tsalikis and Mavrantzas investigated ring linear threading events by an atomistic MD-simulation on PEO ring−linear blends in terms of a geometrical analysis.[28] The simulations have been conducted using ring−linear PEO blends of the same size, over a series of molecular

https://doi.org/10.1021/acs.macromol.3c00560
Macromolecules 2023, 56, 7203−7229

lengths and compositions. The simulations reveal the occurrence of multiple threading events. The lifetime of these threadings were found to be up to 10 times longer than the longest ring relaxation time in its own melt. Figure 19 displays the

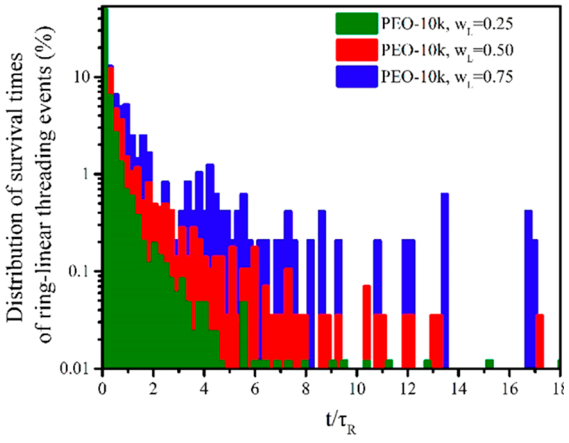

Figure 19. Distribution of lifetimes of ring linear threadings within a symmetric ring-linear blend of 10K PEO for 3 different concentrations of the ring polymers. The time is given in units of the linear PEO Rouse time.[28] Reproduced with permission from ref 28. Copyright 2014 American Chemical Society.

distribution of lifetimes for ring-linear threadings in a symmetric 10K PEO blend for 3 different concentrations of linear chains, clearly revealing exceptionally long ring retardations by the threading events.

Subsequently, the case of a small number of PEO rings in a linear PEO melt was investigated.[143] For these conditions they found that the internal ring dynamics is slaved for longer host linear chains, while in unentangled linear chains, the rings exhibit a Rouse-like dynamics that is faster than the internal dynamics in its own melt. In blends with long, entangled linear chains, the ring dynamics is strongly altered. Its dynamic structure factor $S(Q, t)$ exhibits a steep initial decay up to times on the order of the entanglement time τ_e of the linear host, then for $t > \tau_e$ $S(Q, t)$ becomes practically time-independent approaching Q-dependent plateau values consistent with a neutron spin echo spectroscopy study by Gooßen et al.[136]

Parisi et al. investigated the stress relaxation and zero shear viscosity of symmetric ring-linear blends for ring volume fractions up to $\phi_R = 0.3$.[150] Even though in their own melts rings display a lower viscosity compared to the linear counterpart, in the blends the with increasing ring fraction the viscosity increases above that of the pure linear melt. The phenomenon is believed to origin from ring linear threadings that experience longer lifetimes than the terminal time in the corresponding pure linear melt—the blend can only relax by CR of the threading linear chains. The authors extend the theory by Rubinstein and Colby for CR in linear blends considering the additional contribution from CR processes liberating the rings. The model predicts that the relative viscosity at ring overlap increases in proportion with the square root of the ring mass:

$$\frac{\eta_R(\phi_R^*)}{\eta_L} \approx \phi_R^* \frac{N_R}{N_e} \sim N_R^{1/2} \tag{15}$$

This result demonstrates the possibility to tune linear polymer processing condition in adding a fraction of polymer rings.

By coarse grained MD simulation O'Connor et al. investigated the entanglement topology and extensional rheology of symmetric ring-linear blends across the full composition range.[151] The authors use primitive path analysis, to visualize the structure of the composite entanglement network. While linear chain diffusivity displays little sensitivity toward blending, as ϕ_R decreases ring polymers become heavily threaded by linear chains and eventually are embedded in the linear entanglement network. In this way rings swell by up to 20% and the ring diffusion is reduced by 2 orders of magnitude relative to the pure ring melt.

Finally, by MD simulation and dielectric spectroscopy Mo et al. studied topological effects on the local concentration ϕ_{eff} of segments around a probe segment in linear−linear, ring−linear and ring−ring blends.[149] For linear blends the Lodge−McLeish self-concentration model is supported, while in ring−ring blends chain back bending increases ϕ_{eff} compared to the linear case. In ring−linear blends the strong penetration of rings by linear chains recovers the case of linear blends. These results are supported by dielectric studies on miscible PS/PVME blends of different architecture.

4.6. Challenges for the Future: Ring−Linear Blends. The dynamics of ring−linear blends have been by far less investigated compared to pure ring melts. The available dynamic studies to a significant amount focused on rheological and diffusional properties in such blends. For large enough rings diffusion of rings in such blends is governed by ring−linear threadings. The interpenetration of linear chains into the ring leads to long living constraints that restrain ring mobility. Such threadings were characterized by geometrical analysis displaying a large distribution of threading amounts and lifetimes. Diffusion is thought to take place via constraint release processes, where the multiply treading chains must leave the ring contour. Other than expected large rings immersed in long entangled linear hosts appear to show two distinct diffusion modes. Apart from one study[136] the internal segmental dynamics of rings in linear melts has not been touched. Concerning rheological properties blending linear melts with ring seems to be a novel path to tune linear—as well as nonlinear rheological properties.

Starting with the segmental dynamics of rings in the blend, a thorough investigation across the full volume fraction regime on large rings in long entangled linear hosts needs to be performed. Such investigations will provide insight on the multiple interactions of the threaded ring with the interpenetrating linear chains.

On the side of simulation most of the blend systems were symmetric looking on ring-linear systems of identical molecular weights. As the PFG-NMR studies on asymmetric blends revealed, novel phenomena might be found in simulations of such systems.

The mystery of the two diffusive modes in long chain ring−linear blends needs to be lifted. It would be important to investigate a chemically different ring−linear system, to proof the generic character of the two diffusion modes. Do simulations miss the two-mode structure because the investigated systems are not large enough?

As recently found in simulations, both linear viscoelasticity and nonlinear rheological properties are very complex and might bear surprises for the future. For example, the coupling of ring−linear topologies leads to an intermediate maximum of the zero shear viscosity as a function of ring volume fraction[151] or under elongational flow a strong stress overshoot is predicted. The

https://doi.org/10.1021/acs.macromol.3c00560
Macromolecules 2023, 56, 7203−7229

subject lays outside the frame of this paper but should be kept in mind in future investigations.

Another challenge are ring−ring blends, which were largely overlooked so far. Certainly, these are much harder to realize, in particular experimentally, but should provide a better understanding of the impact of the surrounding melt of rings on the diffusion of individual rings.

Finally, we note that beyond the importance of the discussed findings for synthetic polymers we expect that the results might have important implications also for biological systems such as the organization of chromatin in the cell nucleus[152] or the stabilization of protein structures.[153]

5. TOPOLOGICAL GLASS TRANSITION

5.1. The Role of Threading. An intriguing aspect of ring polymer dynamics relates to the possibility of a topological glass transition, where the dynamical arrest does not occur on the level of the monomeric polymer building blocks but on the scale of the chain size and beyond. In terms of large scale MD-simulations on polymer rings embedded in a gel structure, Michieletto et al. realized that in concentrated solution inter-ring threadings of nonconcatenated ring polymers might lead to a percolating network of interpenetrated rings, where the lifetime of the threadings increase with ring size, ultimately leading to a topologically jammed state.[154]

Then in 2016 these phenomena were further developed toward a theory of topological glass formation in dense ring polymer systems.[25] In pinning randomly a small ring fraction again by MD-simulations Michieletto and Turner established evidence for a transition to a kinetically arrested state, a phenomenon not observed for linear polymers. They attributed the transition to inter-ring topological interactions or threadings that for very large rings may spontaneously lead to an arrested state even without pinning.

It was shown that the number of threadings scales extensively with the ring mass and therefore is larger for large rings. On different scales the threadings establish a hierarchical sequence of constraints that can span the entire system such that the network of constraints can eventually suppress the translational degrees of freedom of the rings. The constraint of uncrossability between chains then creates topological hindrance for the motion of the rings leading to an important slowdown of motion. This retardation increases with the length of rings.

Random pinning of a fraction of rings creates a field of quenched disorder leading to kinetical arrest. For large rings even a small number of such pinned regions is inducing arrest, because the network by threadings is percolating even for a small number of pinned regions. To assess the impact of kinetical hindrance, it was important to study the lifetime of the threadings. Decorrelation of rings takes place when their contact spheres separate. The authors found that the decorrelation functions of the threadings are stretched exponentials with exponents β from 1 for small rings to 1/2 for the largest ring investigated. The corresponding Kohlrausch−Williams−Watts (KWW) times increase exponentially with ring size. Furthermore, it was found that long lasting ring−ring correlations survive even after rings have moved beyond their own size. Tracking the dynamics of unfrozen rings, it was realized that threading also slows down the unfrozen rings. They become caged, while corresponding linear polymers are more or less unaffected. In turn this observation was taken as direct evidence for the existence of threading events. As discussed above, another method to observe threadings was employed by the Mavrantzas group, who performed a geometrical analysis of the simulated ring ensembles.

Varying the fraction of pinned regions, displayed the existence of a critical frozen fraction c_f, above which all unfrozen rings are caged leading to a topological glass transition of the unfrozen rings. As a criterion for c_f the freezing of the translational diffusion coefficient is used.

$$D_{\text{eff}}(c_f) \equiv \lim_{t\to\infty} \langle g_3(t)\rangle/6t \to 0 \tag{16}$$

Thereby $g_3(t)$ is the COM correlation function. Going to larger rings the decay of $D_{\text{eff}}(c)$ becomes increasingly steeper and c_f becomes smaller.

We note that the topological glass transition in ring melts is of very different nature than that in ordinary liquids or linear polymers were freezing occurs on the level of the molecule or monomer, respectively. Since locally the motion of the ring monomers is nearly unaffected, at large momentum transfers Q the dynamic structure factor $S(Q, t)$ of the unfrozen rings is predicted to decay rapidly, while at small Q the decay will be frozen. Thus, the threadings control mainly the small wavenumber modes. In this sense threadings decouple the displacements involving the COM from the internal degrees of freedom. The authors hypothesize that this separation might be the reason, why in the shear modulus $G(t)$ the plateau, characteristic for linear polymers, is replaced by a power low decay. At intermediate time the modulus relates to internal rearrangements, which are unaffected by the topological arrest. Bringing together all simulation results the authors proposed a dynamic phase diagram, which as a function of the pinned fraction separates liquid and glassy behavior. One can see that with increasing molecular weight (small $1/M$ on the Figure 20) the glass transition takes place at a decreasing fraction of pinned rings.

The blue glass transition line is the result from a fit with a phenomenological obtained exponential $N^* = N_g \exp[-3.3c]$, where N^* is the number of beads making up the ring and c is the pinned fraction and $N_g \approx 3500$; p_r is the probability to find an uncaged ring at a 95% confidence interval obtained from a

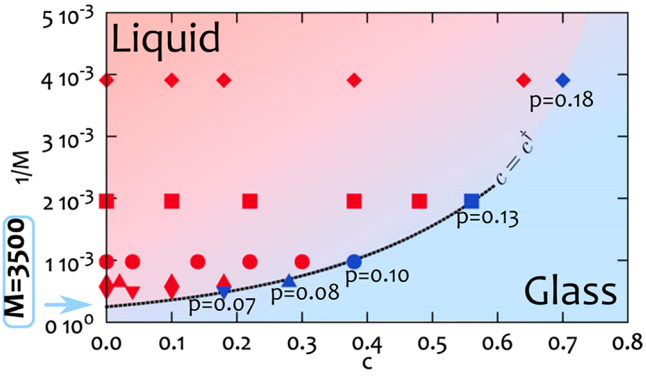

Figure 20. Figure shows the phase space $(1/M, c)$ for systems of rings with length M, in which a fraction c of rings are permanently frozen in space and time. The transition line $(1/M_p c_f)$ is shown together with an exponential fit (dotted line). The colored data points in the diagram indicate whether the system displays a finite diffusion coefficient at large time (red) or whether it is irreversibly caged with vanishing D_{eff} (blue). Along the transition line, the value of the probability p of finding an uncaged ring in any one test performed at fixed c is presented.[25] Reproduced with permission from ref 25. Copyright 2016 National Academy of Science.

https://doi.org/10.1021/acs.macromol.3c00560
Macromolecules 2023, 56, 7203−7229

binomial distribution $(1-p_r)^{(1-c_f)M} = 0.05$, where M is the number of rings in the ensemble. Thus, large ring systems appear to be very sensitive to a small amount of pinning that drives the system to a dynamical arrest. It in some way relates to the cooperativity ideas behind the common glass transition.[155]

The phase diagram suggests that with decreasing $1/N$ finally spontaneous vitrification takes place. Considering N_g as the theoretical ring size upon which spontaneous arrest takes place the relation between c_f and N was further specified as[156]

$$c_f = -f_N \log\left[\frac{N}{N_g}\right] \tag{17}$$

where N_g is the theoretical bead number required for spontaneous vitrification and f_N is a nonuniversal prefactor. Similarly, also the dependence of vitrification on the ring volume fraction in concentrated solutions was studied showing a very similar relationship as above.

$$c_f(\rho, N) = -f_p \log\left[\frac{\rho}{\rho_g(N)}\right] \tag{18}$$

where ρ_g is the corresponding theoretical volume fraction above which for a given M vitrification sets in. ρ_g and N_g are related by

$$\rho_g(N) \sim N^{-\eta} N_g(\rho) \sim \rho^{1/\eta} \text{ with } \eta = \frac{f_N}{f_\rho} = 0.68 \tag{19}$$

yielding a universal function for the theoretical glass line.

Finally, they note that in concentrated ring solutions and melts dynamic heterogeneity or non-Gaussian dynamics is resulting from clustering into distinct fast and slow moving components.

Roy et al. investigated the effect of polymer stiffness and pressure on the topological vitrification of dense ring systems. Stiffer rings get more easily arrested at lower pressures. While flexible rings at ambient pressure only arrest for large N at a reasonably low pinning fraction, stiffer rings are already affected at smaller sizes. The authors presented a phenomenology of ring conformations under pressure and stiffness: flexible rings deform to crumbled globules, semi flexible rings tend to assume rod-like shape, while stiff rings form elongated plate like conformations transforming under pressure to circular shapes promoting clustering. For all stiffnesses pressure promotes threading that slows down the dynamics and the lifetime of threading events increases with pressure.

Combining the observed structural and dynamical properties, the simulations show the spontaneous emergence of slow, glassy dynamics in ring polymer systems. By suitable selection of ring polymer stiffness and pressures, slow dynamics can be induced in ring polymers at low pressure values. The formation of such topologically constrained states were also observed for relatively small ring sizes compared to what has been explored earlier, indicating that the access to such states can be obtained by tuning the properties of the ring.

Very recently J. Li et al.[157] investigated the glass formation of mechanically interlocked rings on the nanometer-scale using molecular dynamics simulations. They found that decreasing the chain length in the mechanically interlocked system is equivalent to inducing an effective chain stiffness on the subrings, which provides an explanation for the transient dynamic arrest in the system of interlocked rings with rather short chains.

5.2. Topological Volume. Considering the similarity of ring systems with soft colloids a very different approach based on a topological free volume (TFV) was taken by Sakaue.[26] For linear polymers the number X of interpenetrating chains with a given chain is extensive:

$$X \sim \frac{R^3}{(l^3 N)} \quad l^3 N^{3/2}/(l^3 N) \sim N^{1/2} \tag{20}$$

where $R = lN^{1/2}$ is the chain radius and l the segment or monomer length. X grows unrestrictedly with an increase of N. The large interpenetration leads to entanglements that restrict lateral chain motion and promotes reptation, where chain ends play an essential role. For large enough rings, where $R \sim N^{1/3}$ holds, following eq 20 X becomes constant, even though $X \gg 1$. Thus, for rings a soft particle picture holds that, however, allows for much overlap. The related topological constraints (TC) are qualitatively different from those for linear polymers. As is intuitively evident, the TC impose entropic repulsion on a given ring against the surrounding rings. The distance between rings $r \sim R/X^{1/3}$ looks like the interparticle distance in systems of rigid particles and the effect of TC may be treated as in liquids and glass transition physics. Comparing the inter-ring distance $r \cong R/X^{1/3}$ with the distance between rigid colloidal particles at a volume fraction ψ: $r \cong b/\psi^{1/3}$, we have $r > R$ for rigid colloids but $r < R$ for interpenetrating rings. Realizing the connection between ordinary colloidal and ring physics, facilitates the application of colloidal physics including glass transition exploits for an understanding of the physics of ring systems.

Relating to ordinary glass transition physics, the ring length N replaces the temperature T. Since rings are built from elementary loops of size N_e, there is a limiting scale toward small N: $X_e \equiv X(N = N_e) \sim R_e^3/(N_e a^3) \sim N_e^{1/2}$. For typical N_e between 50 and 100:7 < X_e < 10. The key difference to ordinary liquids or colloids is that rings can penetrate each other strongly such that the radius R is much larger than the quantity that would arise from the ring volume fraction $\psi \equiv X/X_c$. X_c is the maximum number of interpenetrating rings that is achieved in the limit of large N. ψ then is termed as the topological volume fraction. With this in place a phenomenological free energy F may be constructed

$$\frac{F}{k_B T} = -\ln(1-\psi) + \frac{N}{N_e}\left(\frac{X_e}{X}\right)^{1/(3\nu_0 - 1)} \tag{21}$$

The first term favors smaller topological volume fractions, while the second term is the penalty for ring squeezing and would prefer larger rings. For the discussion of the exponent $\nu_0 \cong 0.588$, the critical exponent for a self-avoiding chain, see the original paper. The minimization of F gives $R(N)$ as a universal function of N/N_e. Figure 21 compares the result with simulations by Vettorel, Halverson and Michieletto. Nearly perfect agreement is achieved: R/R_e up to $N/N_e \approx 30-40$ follows a power law with $\nu \cong 2/5$. The crossover to $\nu = 1/3$ is hardly visible even for the largest $N/N_e \approx 60$ (Figure 21b). Figure 20a displays the interpenetration number X/X_e as a function of N/N_e. Also, the simulation results are included. Again, very good agreement with simulation results is found. We note that beyond X_e at $N = N_e$ the penetration number for very large rings increases by less than a factor of 2.

Using the relationship between colloidal and ring physics, the cooperative dynamics of the ring system may be estimated. The basic time becomes the Rouse time of the elementary loop $\tau_e \sim \tau_0 N_e^2$. For solid particles structural arrest occurs at a critical volume fraction ψ_c, because the particles cannot interpenetrate. In contrast for rings the centers of mass can fully overlap in space leading to growing cooperativity for volume fractions $\psi \geq \psi_e$

https://doi.org/10.1021/acs.macromol.3c00560
Macromolecules 2023, 56, 7203−7229

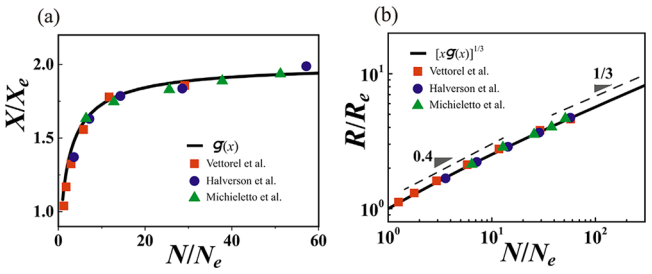

Figure 21. Comparison of free energy prediction (solid line) with numerical simulation data for the coordination number X (a) and spatial size R (b) of rings in dense solution of nonconcatenated rings. Numerical data are obtained from literature (squares,[9] circles,[15] triangles[25]). Before reaching the asymptotic compact scaling with $\nu = 1/3$, there exists a broad crossover, which may be fit reasonably well by an effective exponent $\nu_{\text{eff}} \simeq 0.4$.[26] Reproduced with permission from ref 26. Copyright 2018 Elsevier B.V. Reprinted in part with permission from ref 9. Copyright 2010 IOP Publishing. Reprinted in part with permission from ref 15. Copyright 2011 AIP Publishing. Reprinted in part with permission from ref 16. Copyright 2012.

where $\psi_e = X_e/X_c$ and X_c is the limiting value for large N/N_e. The global structural relaxation time is predicted to grow with a power law in N/N_e, which in the large N limit becomes $\tau \sim \left(\frac{N}{N_e}\right)^{z_{\text{eff}}}$ with $z_{\text{eff}} \cong 3$. Evaluating the COM diffusion as $D_{\text{com}}(N) \sim R(N)^2/\tau(N)$ reveals $D_{\text{com}} \sim N^{-\cong 2.3}$ in very good agreement with simulations and PFG-NMR measurements on PEO rings. We note that (i) scaling theories generally lead to exponents below 2 and (ii) the assumption of full overlap leads to a power law slowing down but not to dynamical arrest.

5.3. Microscopic Theory. The Schweizer group formulated a microscopic theory at the level of forces between segments for the COM motion of ring polymers putting together ideas from polymer, colloid, and liquid statistical physics.[158] They started from static topological effects occurring on the level of intra- and inter-ring segmental pair correlation functions. Thereby, higher order correlations leading, e.g., to threading effects were not addressed. The approach relates caging effects to the segmental scale repulsive forces that also determine friction. The core idea is that slow ring COM dynamics is causally related to structural pair correlations via a dynamic caging mechanism formulated at the segmental level, where forces act.

The theory predicts a breakdown of the Rouse theory related to length scale-dependent temporal correlation of forces exerted on pairs of tagged ring segments from surrounding polymers. At large enough degrees of polymerization (N), the scaling of the COM diffusion constant $D_{\text{com}} \propto N^{-2}$ is predicted. The crossover size N_D is related to the product of the macromolecular volume fraction and a dimensionless compressibility. Furthermore, the intermediate time COM transport is described in terms of a generalized Langevin equation. Because of the self-similar internal ring structure non−Fickian transport is predicted with two subdiffusive regimes.

Figure 22a displays the dimensionless COM MSD in units of the radius of gyration for melts of different sized rings as a function of the reduced r/τ_0 time ($\tau_0 = \frac{k_B T}{\xi_0 l^2}$, with ξ_0 the monomeric friction coefficient and l the monomer length). The intermediate time subdiffusive regime preceding Fickian diffusion displays a power law in time with an exponent that diminishes with increasing size. For the largest ring $\langle R^2_{\text{com}} \rangle \sim t^{1/2}$ is assumed.

However, a larger interval with constant time exponents does not exist, but the apparent exponent changes with time and depends strongly on the ring size N. Figure 22b displays the exponent γ for different ring sizes as a function of reduced MSD. From early times γ starts at unity (short-time Rouse diffusion), then decreases to a minimum value that becomes smaller with growing N and then for long times again increases to unity, when the Fickian regime is reached.

Given that polymer rings are unusual (ultrasoft) objects, with this approach a crossover to activated motion and a kinetic glass transition is not a priori assured. Future developments might lead to a microscopic theory of strong self-consistent caging effects, activated dynamics, and kinetic vitrification under both quiescent and quenched disorder pinning conditions.

5.4. Challenges for the Future. We have presented three different approaches to deal with the slowing down of motion in large ring systems including the possibility of kinetic arrest. The first starts from the idea of threadings that develop a percolating network, with the consequence that pinning a small fraction of rings by the network connectivity the whole is driven into kinetic arrest. The topological volume idea dwells on the similarity of rings and soft colloids. Each ring is surrounded by a stable finite number of other rings that form a cage. However, since rings may fully interpenetrate each other, this cage does not lead to

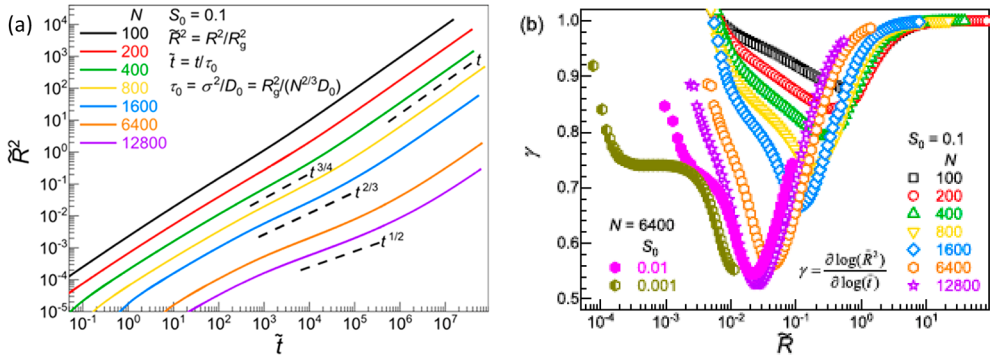

Figure 22. (a) Dimensionless ring COM MSD in units of the mean square radius of gyration as a function of reduced segmental time (units of the elementary time scale τ_0) for a wide range of N values and a typical melt value of dimensionless compressibility $S_0 = 0.1$. (b) Time evolution of the effective temporal power law scaling exponent for the ring COM MSD data presented in (a): $\gamma = \partial \log(\tilde{R}_2)/\partial \log(t)$. Most results are for $S_0 = 0.1$ as in (a), with two examples shown for much smaller values at fixed $N = 6400$. The apparent exponent is plotted vs reduced mean displacement $\tilde{R}(t) = R(t)/R_g$.[158] Reproduced with permission from ref 158. Copyright 2020 American Chemical Society.

https://doi.org/10.1021/acs.macromol.3c00560
Macromolecules 2023, 56, 7203−7229

kinetical arrest but rather to a power law slowing down of the diffusivity. Finally, a microscopic theory basing on generalized Langevin equations again predicts significant slowing down however not yet a glass transition. On the experimental side, only studies dealing with caging as possible precursor for a glass transition exists. In this work a well pronounced non-Gaussian behavior of the COM diffusion was detected that showed analogies to the cage effect known from glassy systems.

Given the different theoretical approaches and the missing experimental results a lot of future efforts are needed:

The first and to us most important issue relates to an experimental verification of a topological glass transition in dense ring systems. Such an experimental approach would need to combine diffusion studies on the scale, where Fickian diffusion prevails and experiments on the nanoscale, where the segmental and loop motion is visible.

Given the fact that the different theoretical approaches in some way are always backed by simulations, a crucial task would be to find out how the different approaches connect to each other: (i) The relation of the TFV picture and the threading approach (TA) needs to be clarified; there must be some correspondence between the structural relaxation time in the TFV frame with the ring dethreading time possibly responsible for the slow mode in stress relaxation. (ii) The analogy to soft colloids needs to be further elucidated. Soft colloids are strong glass formers and rings could be viewed as the softest "'particle'" there exist. Looking on the energy scale the repulsive energy between rings is on the level of k_BT, while that, e.g., between star polymers is much higher.[159] Also, rings may overlap easily. (iii) Another issue is a better understanding of cooperativity which is crucial for the slowing down of motion. (iv) A better theoretical foundation of the TFV approach would be desirable. The model builds on the rather speculative cooperative "free volume string" model[160] of relaxation in glass-forming liquids.

From the side of a microscopic approach as provided by the Schweizer group, work in the direction of combining methods of polymer, colloid, and glass physics to create a microscopic theory of strong self-consistent caging effects, activated dynamics, and kinetic vitrification[161−164] under both quiescent and quenched disorder pinning[165] would be desirable.

6. FUTURE PERSPECTIVES

In our survey we have demonstrated that important progress in the understanding of both the conformation as well as the dynamics of polymer ring systems has been achieved. These mainly based on theoretical developments and a very large number of simulations. Unfortunately, due to the difficulties of synthesizing well-defined large ring polymers the experimental scrutiny lags. Here we emphasize the to our opinion most important challenges for future research on ring systems.

To extend the experimental approach novel synthesis routes to create very large well-defined ring polymers based on different monomers are badly needed, as they are the precondition to extend future experimental research.

We now go to the different aspects of fundamental research on polymer rings and present the most needed efforts:

- Concerning the conformation of rings many theories and also simulations consider double folded structures that following recent scrutiny are doubtful; also, such structures have never been observed experimentally. Thus, approaches that are based on lattice animal arguments appear to be questionable and may be an artifact of very long relaxation times of such structures taken as starting conformations in simulations. The question needs to be posed, whether the tree structures found in simulations relate to the initial double folded structures that are imposed as the starting conformations.
- The location and the width of the size dependent transition to mass fractal statistics is unclear and will need further studies. The transition may also be influenced by the local flexibility of the rings. Sakaue[93] predicted that the crossover ring size to compact statistics $R \sim N^{1/3}$ decreases sharply with increasing stiffness, meaning that the topological effects are even more important for worm-like ring chains such as DNA. Systematic investigation on the influence of increased ring stiffness on the conformational properties accompanied by topological glass transitions could transfer the problem in the direction of biology.
- Ring−ring threading appears to govern the terminal relaxation of the dynamic modulus and may initiate a topological dynamical arrest for very large rings. An experimental verification of this novel topological glass transition in dense ring systems appears to us as one of the most important challenges in the realm of ring dynamics. Supporting the notion of a looming glass transition are observations of a cage effect well-known for glass forming liquids.
- The degree of cooperativity of motion is another very interesting issue: Using a novel dynamical entanglement analysis (DEA) Michieletto and Sakaue opened the way to quantitatively study dynamic correlations between pairs of polymers albeit rings on the level of diffusion. In the future it would be interesting to study such cooperativity on the monomer or even better on the level of entanglement strands.
- Different theoretical approaches seem to be always backed by simulations. A crucial task would be to find out how the different approaches connect to each other: (i) The relation of the TFV picture and the threading approach needs to be clarified. (ii) The analogy to soft colloids needs to be further elucidated. Soft colloids are strong glass formers and rings could be viewed as the softest "'particle'" there exist. (iii) Also, a better understanding of cooperativity, which is crucial for the slowing down of motion is called for.
- A systematic study of the miscibility of ring−ring and ring−linear blends is missing. From Sakaue's theory antithetic phenomena are expected: while ring−ring systems are predicted to exhibit reduced miscibility compared to the linear counterpart, ring−linear blend are expected to show the opposite behavior of an importantly increased miscibility. Systematic investigations of entropy of mixing vs $N_{e,0}$ performed on different rings are required. Experimental investigations are largely missing.
- With one exception microscopic results on the ring dynamics in ring−linear blends are entirely missing. Starting with the segmental dynamics of rings in the blend with linear polymers, a thorough investigation across the full volume fraction regime on large rings in long entangled linear hosts needs to be performed. Such investigations will provide insight on the multiple interactions of the threaded rings with the interpenetrating linear chains. On the side of simulation most of the

https://doi.org/10.1021/acs.macromol.3c00560
Macromolecules 2023, 56, 7203−7229

studied blend systems were symmetric looking on ring-linear systems of identical molecular weights. As the PFG-NMR studies on asymmetric blends revealed, novel phenomena might be found in simulations on such systems.

- The mystery of the two diffusive modes in long chain ring-linear blends needs to be lifted. It would be important to investigate a chemically different ring-linear system, to proof the generic character of the two diffusion modes. Do simulations miss the two-mode structure because the investigated systems are not large enough?

Finally, we note that beyond the importance of the discussed findings for synthetic polymers we expect that the results might have important implications also for biological systems such as the organization of chromatin in the cell nucleus[152] or the stabilization of protein structures.[166]

AUTHOR INFORMATION

Corresponding Author

Margarita Kruteva − *Jülich Centre for Neutron Science (JCNS-1) and Institute for Biological Information Processing (IBI-8), Forschungszentrum Jülich GmbH, 52428 Jülich, Germany;* orcid.org/0000-0002-7686-0934; Email: m.kruteva@fz-juelich.de

Authors

Jürgen Allgaier − *Jülich Centre for Neutron Science (JCNS-1) and Institute for Biological Information Processing (IBI-8), Forschungszentrum Jülich GmbH, 52428 Jülich, Germany;* orcid.org/0000-0002-9276-597X

Dieter Richter − *Jülich Centre for Neutron Science (JCNS-2) and Peter Grünberg Institute (PGI-4), Forschungszentrum Jülich GmbH, 52428 Jülich, Germany*

Complete contact information is available at: https://pubs.acs.org/10.1021/acs.macromol.3c00560

Notes

The authors declare no competing financial interest.

Biographies

Dr. Margarita Kruteva Margarita Kruteva received her PhD in Physics in 2003 from Kazan State University, Russia. From 2005 she worked as a postdoc at the University of Leipzig on exchange processes in nanoporous materials using PFG NMR. At the Research Centre Jülich (FZJ) she started as EU sponsored postdoc studying polymer dynamics confined in nanoporous materials using high resolution neutron spectroscopy. Since 2013 she has been a senior scientist at the Jülich Centre for Neutron Science (JCNS) at Forschungszentrum Jülich. Her research interest focuses on structure and dynamics of polymers and complex macromolecular systems by scattering methods and PFG NMR.

Dr. Jürgen Allgaier Jürgen Allgaier received his PhD in Chemistry in 1993 at the University of Freiburg, Germany. He worked as a postdoc at the University of Sheffield, U.K. on the synthesis of nonlinear model polymers using anionic polymerization techniques. In 1995 he joined the Research Centre Jülich. At the Jülich Centre for Neutron Science his present research interests are in the areas of anionic polymerization, polymers with architecture, and cyclic polymers. Further research fields include supramolecular polymers, polymer−particle composites, and polymer−lipid interactions as well as the development of deuteration techniques for polymers and organic compounds.

Prof. em. Dr. Dieter Richter Dieter Richter received his PhD (1977) at the RWTH Aachen, Germany. After postdoc at Brookhaven National Laboratory, Habilitation (1983) and group leader at the ILL in Grenoble (1985-89), he was appointed as director of neutron scattering within the IFF at FZJ in Jülich, Germany. From 2011 to 2015 he served as Scientific Director at the Munich FRM2 research reactor. Since retirement he has worked as an advisor for the FZJ. Co-authoring more than 600 papers, (about 25 000 citations), he received several high-ranking awards. He was member and chairperson of many scientific panels and founded the European Neutron Scattering Association and the European Network of Excellence "SoftComp". His current interests are the structure and dynamics of macromolecular soft and biological systems.

NOMENCLATURE

BMF	Bond fluctuation model
C_∞	Characteristic ratio
CD	Cates and Deutsch model
COM	Center of mass
CR	Constraint release

https://doi.org/10.1021/acs.macromol.3c00560
Macromolecules 2023, 56, 7203−7229

DEA	Dynamical entanglement analysis
$D_{R,e}$	Rouse diffusion coefficient of one elementary loop
d_b	Fractal dimension of the backbone
d_f	Fractal dimension
d_{tube}	Reptation tube diameter
DFLA	Double folded lattice animal
FLG	Fractal loopy globule
l	Monomer length
L	Length of the backbone
l_0	Bond length
LCCC	Liquid chromatography at critical condition
LP	Linear polymer
MALDI-TOF	Matrix-assisted laser-desorption time-of-flight mass spectroscopy
MC	Monte Carlo
MD	Molecular dynamics
M_e	Entanglement molecular weight
MSD	Mean squared displacement
M_w	Molecular weight
MWD	Molecular weight distribution
n_b	Number of main chain bonds in a monomer
N_e	Number of monomers within an entanglement strand
$N_{e,0}$	Elementary loop size: $N_{e,0} \cong N_e$
n_P	Number of linear chain interpenetrations in a ring-linear blend
NG	Non-Gaussian
NSE	Neutron Spin Echo
O_{KN}	Kavassalis-Noolandi overlap parameter
PB	Polybutadiene
PDMS	Polydimethylsiloxane
PE	Polyethylene
PEO, PEG	Poly(ethylene oxide), poly(ethylene glycol); differ by end groups
PI	Polyisoprene
PS	Polystyrene
PVME	Poly(vinyl methyl ether)
r_e	Diameter of a ring loop
SANS	Small angle neutron scattering
SAXS	Small angle X-ray scattering
SEC	Size exclusion chromatography
TC	Topological constraint
TFV	Topological free volume
X	Number of interpenetrating chains
η_0	Zero-shear viscosity
μ	Spectral exponent
v_0	Monomer volume
τ_d	Terminal time
τ_e	Entanglement time
τ_p	Rouse relaxation time for mode p
χ^2	Mean squared error
$\chi_{F,RL}$	Flory–Huggins parameter for a ring-linear blens

REFERENCES

(1) Doi, M.; Edwards, S.F.. *The Theory of Polymer Dynamics*; Clarendon Press: Oxford, 1986.

(2) Richter, D.; Monkenbusch, M.; Arbe, A.; Colmenero, J. *Neutron Spin Echo in Polymer Systems*; Springer: Berlin, Heidelberg, 2005; Vol. *174*.

(3) de Gennes, P. G. Reptation of a Polymer Chain in the Presence of Fixed Obstacles. *J. Chem. Phys.* **1971**, *55* (2), 572–579.

(4) McLeish, T. C. B. Tube Theory of Entangled Polymer Dynamics. *Adv. Phys.* **2002**, *51* (6), 1379–1527.

(5) Freifelder, D.; Kleinschmidt, A. K.; Sinsheimer, R. L. Electron Microscopy of Single-Stranded DNA: Circularity of DNA of Bacteriophage ΦX174. *Science (80-.)* **1964**, *146* (3641), 254–255.

(6) Craik, D. J. Seamless Proteins Tie up Their Loose Ends. *Science* **2006**, *311* (5756), 1563–1564, DOI: 10.1126/science.1125248.

(7) Grosberg, A. Y.; Nechaev, S. K.; Shakhnovich, E. I. The Role of Topological Constraints in the Kinetics of Collapse of Macromolecules. *J. Phys. (Paris)* **1988**, *49* (12), 2095–2100.

(8) Cates, M. E.; Deutsch, J. M. Conjectures on the Statistics of Ring Polymers. *J. Phys. Paris* **1986**, *47* (12), 2121–2128.

(9) Vettorel, T.; Grosberg, A. Y.; Kremer, K. Statistics of Polymer Rings in the Melt: A Numerical Simulation Study. *Phys. Biol.* **2009**, *6* (2), No. 025013.

(10) Müller, M.; Wittmer, J. P.; Cates, M. E. Topological Effects in Ring Polymers. II. Influence of Persistence Length. *Phys. Rev. E - Stat. Physics, Plasmas, Fluids, Relat. Interdiscip. Top.* **2000**, *61* (4), 4078–4089.

(11) Müller, M.; Wittmer, J. P.; Barrat, J. L. On Two Intrinsic Length Scales in Polymer Physics: Topological Constraints vs. Entanglement Length. *Europhys. Lett.* **2000**, *52* (4), 406–412.

(12) Brown, S.; Szamel, G. Computer Simulation Study of the Structure and Dynamics of Ring Polymers. *J. Chem. Phys.* **1998**, *109* (14), 6184.

(13) Müller, M.; Wittmer, J. P.; Cates, M. E. Topological Effects in Ring Polymers: A Computer Simulation Study. *Phys. Rev. E - Stat. Physics, Plasmas, Fluids, Relat. Interdiscip. Top.* **1996**, *53* (5), 5063–5074.

(14) Lieberman-Aiden, E.; Van Berkum, N. L.; Williams, L.; Imakaev, M.; Ragoczy, T.; Telling, A.; Amit, I.; Lajoie, B. R.; Sabo, P. J.; Dorschner, M. O.; Sandstrom, R.; Bernstein, B.; Bender, M. A.; Groudine, M.; Gnirke, A.; Stamatoyannopoulos, J.; Mirny, L. A.; Lander, E. S.; Dekker, J. Comprehensive Mapping of Long-Range Interactions Reveals Folding Principles of the Human Genome. *Science (80-.)* **2009**, *326* (5950), 289–293.

(15) Halverson, J. D.; Lee, W. B.; Grest, G. S.; Grosberg, A. Y.; Kremer, K. Molecular Dynamics Simulation Study of Nonconcatenated Ring Polymers in a Melt. I. Statics. *J. Chem. Phys.* **2011**, *134* (20), No. 204904.

(16) Halverson, J. D.; Grest, G. S.; Grosberg, A. Y.; Kremer, K. Rheology of Ring Polymer Melts: From Linear Contaminants to Ring-Linear Blends. *Phys. Rev. Lett.* **2012**, *108* (3), No. 038301.

(17) Kapnistos, M.; Lang, M.; Vlassopoulos, D.; Pyckhout-Hintzen, W.; Richter, D.; Cho, D.; Chang, T.; Rubinstein, M. Unexpected Power-Law Stress Relaxation of Entangled Ring Polymers. *Nat. Mater.* **2008**, *7* (12), 997–1002.

(18) Grosberg, A. Y. Annealed Lattice Animal Model and Flory Theory for the Melt of Non-Concatenated Rings: Towards the Physics of Crumpling. *Soft Matter* **2014**, *10* (4), 560–565.

(19) Kavassalis, T. A.; Noolandi, J. Entanglement Scaling in Polymer Melts and Solutions. *Macromolecules* **1989**, *22* (6), 2709–2720.

(20) Fetters, L. J.; Lohse, D. J.; Richter, D.; Witten, T. A.; Zirkel, A. Connection between Polymer Molecular Weight, Density, Chain Dimensions, and Melt Viscoelastic Properties. *Macromolecules* **1994**, *27* (17), 4639–4647, DOI: 10.1021/ma00095a001.

(21) Kruteva, M.; Allgaier, J.; Monkenbusch, M.; Porcar, L.; Richter, D. Self-Similar Polymer Ring Conformations Based on Elementary Loops: A Direct Observation by SANS. *ACS Macro Lett.* **2020**, *9* (4), 507–511.

(22) Kruteva, M.; Monkenbusch, M.; Allgaier, J.; Holderer, O.; Pasini, S.; Hoffmann, I.; Richter, D. Self-Similar Dynamics of Large Polymer Rings: A Neutron Spin Echo Study. *Phys. Rev. Lett.* **2020**, *125* (23), No. 238004.

(23) Tsalikis, D. G.; Mavrantzas, V. G.; Vlassopoulos, D. Analysis of Slow Modes in Ring Polymers: Threading of Rings Controls Long-Time Relaxation. *ACS Macro Lett.* **2016**, *5* (6), 755–760.

(24) Smrek, J.; Kremer, K.; Rosa, A. Threading of Unconcatenated Ring Polymers at High Concentrations: Double-Folded vs Time-Equilibrated Structures. *ACS Macro Lett.* **2019**, *8* (2), 155–160.

https://doi.org/10.1021/acs.macromol.3c00560
Macromolecules 2023, 56, 7203–7229

(25) Michieletto, D.; Turner, M. S. A Topologically Driven Glass in Ring Polymers. *Proc. Natl. Acad. Sci. U. S. A* **2016**, *113* (19), 5195−5200.
(26) Sakaue, T. Statistical Physics of Ring Polymers Based on Topological Volume Concept. *React. Funct. Polym.* **2019**, *134*, 150−155.
(27) Sakaue, T. Ring Polymers in Melts and Solutions: Scaling and Crossover. *Phys. Rev. Lett.* **2011**, *106* (16), No. 167802.
(28) Tsalikis, D. G.; Mavrantzas, V. G. Threading of Ring Poly(Ethylene Oxide) Molecules by Linear Chains in the Melt. *ACS Macro Lett.* **2014**, 3 (8), 763−766.
(29) Kruteva, M.; Allgaier, J.; Richter, D. Direct Observation of Two Distinct Diffusive Modes for Polymer Rings in Linear Polymer Matrices by Pulsed Field Gradient (PFG) NMR. *Macromolecules* **2017**, *50* (23), 9482−9493.
(30) Gooßen, S.; Brás, A. R.; Krutyeva, M.; Sharp, M.; Falus, P.; Feoktystov, A.; Gasser, U.; Pyckhout-Hintzen, W.; Wischnewski, A.; Richter, D. Molecular Scale Dynamics of Large Ring Polymers. *Phys. Rev. Lett.* **2014**, *113* (16), No. 168302.
(31) Endo, K. Synthesis and Properties of Cyclic Polymers. *Adv. Polym. Sci.* **2008**, *217* (1), 121−183.
(32) Laurent, B. A.; Grayson, S. M. Synthetic Approaches for the Preparation of Cyclic Polymers. *Chem. Soc. Rev.* **2009**, *38* (8), 2202−2213.
(33) Ochs, J.; Pagnacco, C. A.; Barroso-Bujans, F. Macrocyclic Polymers: Synthesis, Purification, Properties and Applications. *Prog. Polym. Sci.*. Pergamon,November 1, **2022**; p 101606.*134*
(34) Kricheldorf, H. R. Cyclic Polymers: Synthetic Strategies and Physical Properties. *J. Polym. Sci. Part A Polym. Chem.* **2010**, *48* (2), 251−284.
(35) Jia, Z.; Monteiro, M. J. Cyclic Polymers: Methods and Strategies. *J. Polym. Sci. Part A Polym. Chem.* **2012**, *50* (11), 2085−2097.
(36) Brown, H. A.; Waymouth, R. M. Zwitterionic Ring-Opening Polymerization for the Synthesis of High Molecular Weight Cyclic Polymers. *Acc. Chem. Res.* **2013**, *46* (11), 2585−2596.
(37) Chang, Y. A.; Waymouth, R. M. Recent Progress on the Synthesis of Cyclic Polymers via Ring-Expansion Strategies. *J. Polym. Sci. A: Polym. Chem.* **2017**, *55* (18), 2892−2902, DOI: 10.1002/pola.28635.
(38) Haque, F. M.; Grayson, S. M. The Synthesis, Properties and Potential Applications of Cyclic Polymers. *Nature Chem.* **2020**, *12*, 433−444, DOI: 10.1038/s41557-020-0440-5.
(39) Chen, C.; Weil, T. Cyclic Polymers: Synthesis, Characteristics, and Emerging Applications. *Nanoscale Horizons*. The Royal Society of Chemistry September 26, 2022; pp 1121−1135.
(40) Kricheldorf, H. R.; Weidner, S. M. The Ring-Opening Polymerization−Polycondensation (ROPPOC) Approach to Cyclic Polymers. *Macromol. Rapid Commun.* **2020**, *41* (14), No. 2000152.
(41) Yoon, K. Y.; Noh, J.; Gan, Q.; Edwards, J. P.; Tuba, R.; Choi, T. L.; Grubbs, R. H. Scalable and Continuous Access to Pure Cyclic Polymers Enabled by 'Quarantined' Heterogeneous Catalysts. *Nat. Chem. 2022 1411* **2022**, *14* (11), 1242−1248.
(42) Roovers, J.; Toporowski, P. M. Synthesis and Characterization of Ring Polybutadienes. *J. Polym. Sci., Part B: Polym. Phys.* **1988**, *26* (6), 1251−1259.
(43) Roovers, J.; Toporowski, P. M. Synthesis of High Molecular Weight Ring Polystyrenes. *Macromolecules* **1983**, *16* (6), 843−849.
(44) Sharma, S.; Ntetsikas, K.; Ladelta, V.; Bhaumik, S.; Hadjichristidis, N. Well-Defined Cyclic Polymer Synthesis via an Efficient Etherification-Based Bimolecular Ring-Closure Strategy. *Polym. Chem.* **2021**, *12* (45), 6616−6625.
(45) Cho, D.; Masuoka, K.; Koguchi, K.; Asari, T.; Kawaguchi, D.; Takano, A.; Matsushita, Y. Preparation and Characterization of Cyclic Polystyrenes. *Polym. J. 2005 377* **2005**, *37* (7), 506−511.
(46) Quirk, R. P.; Wang, S. F.; Foster, M. D.; Wesdemiotis, C.; Yol, A. M. Synthesis of Cyclic Polystyrenes Using Living Anionic Polymerization and Metathesis Ring-Closure. *Macromolecules* **2011**, *44* (19), 7538−7545.
(47) Schappacher, M.; Deffieux, A. α-Acetal-ω-Bis(Hydroxymethyl) Heterodifunctional Polystyrene: Synthesis, Characterization, and Investigation of Intramolecular End-to-End Ring Closure. *Macromolecules* **2001**, *34* (17), 5827−5832.
(48) Kobayashi, Y.; Doi, Y.; Abdul Rahman, S. S.; Kim, E.; Kim, T.-H.; Takano, A.; Matsushita, Y. SANS Study of Ring Topology Effects on the Miscibility of Polymer Blends. *Macromolecules* **2018**, *51* (5), 1885−1893.
(49) He, Q.; Yol, A. M.; Wang, S. F.; Ma, H.; Guo, K.; Zhang, F.; Wesdemiotis, C.; Quirk, R. P.; Foster, M. D. Efficient Synthesis of Well-Defined Cyclic Polystyrenes Using Anionic Polymerization, Silicon Chloride Linking Chemistry and Metathesis Ring Closure. *Polym. Chem.* **2016**, *7* (37), 5840−5848.
(50) Zaldua, N.; Liénard, R.; Josse, T.; Zubitur, M.; Mugica, A.; Iturrospe, A.; Arbe, A.; De Winter, J.; Coulembier, O.; Müller, A. J. Influence of Chain Topology (Cyclic versus Linear) on the Nucleation and Isothermal Crystallization of Poly(l -Lactide) and Poly(d -Lactide). *Macromolecules* **2018**, *51* (5), 1718−1732.
(51) Ochs, J.; Veloso, A.; Martínez-Tong, D. E.; Alegria, A.; Barroso-Bujans, F. An Insight into the Anionic Ring-Opening Polymerization with Tetrabutylammonium Azide for the Generation of Pure Cyclic Poly(Glycidyl Phenyl Ether). *Macromolecules* **2018**, *51* (7), 2447−2455.
(52) Antonini Vitali, C.; Masci, B. Template Effects. 7. Large Unsubstituted Crown Ethers from Polyethylene Glycols: Formation, Analysis, and Purification. *Tetrahedron* **1989**, *45* (7), 2201−2212.
(53) Sun, T.; Yu, G.-E.; Price, C.; Booth, C.; Cooke, J.; Ryan, A. J. Cyclic Polyethers. *Polymer* **1995**, *36* (19), 3775−3778.
(54) Zhang, Y.; Wang, G.; Huang, J. Synthesis of Macrocyclic Poly(Ethylene Oxide) and Polystyrene via Glaser Coupling Reaction. *Macromolecules* **2010**, *43* (24), 10343−10347.
(55) Hövelmann, C. H.; Gooßen, S.; Allgaier, J. Scale-Up Procedure for the Efficient Synthesis of Highly Pure Cyclic Poly(Ethylene Glycol). *Macromolecules* **2017**, *50* (11), 4169−4179.
(56) Kruteva, M.; Allgaier, J.; Monkenbusch, M.; Hoffmann, I.; Richter, D. Structure and Dynamics of Large Ring Polymers. *J. Rheol.* **2021**, *65* (4), 713−727.
(57) Sun, P.; Chen, J.; Liu, J.; Zhang, K. Self-Accelerating Click Reaction for Cyclic Polymer. *Macromolecules* **2017**, *50* (4), 1463−1472.
(58) Zhao, J.; Zhou, Y.; Zhou, Y.; Zhou, N.; Pan, X.; Zhang, Z.; Zhu, X. A Straightforward Approach for the One-Pot Synthesis of Cyclic Polymers from RAFT Polymers via Thiol-Michael Addition. *Polym. Chem.* **2016**, *7* (9), 1782−1791.
(59) Stanford, M. J.; Pflughaupt, R. L.; Dove, A. P. Synthesis of Stereoregular Cyclic Poly(Lactide)s via "Thiol-Ene" Click Chemistry. *Macromolecules* **2010**, *43* (16), 6538−6541.
(60) Lonsdale, D. E.; Bell, C. A.; Monteiro, M. J. Strategy for Rapid and High-Purity Monocyclic Polymers by CuAAC "Click" Reactions. *Macromolecules* **2010**, *43* (7), 3331−3339.
(61) Schulz, M.; Tanner, S.; Barqawi, H.; Binder, W. H. Macrocyclization of Polymers via Ring-Closing Metathesis and Azide/Alkyne-"Click"-Reactions: An Approach to Cyclic Polyisobutylenes. *J. Polym. Sci. Part A Polym. Chem.* **2010**, *48* (3), 671−680.
(62) Goldmann, A. S.; Quémener, D.; Millard, P. E.; Davis, T. P.; Stenzel, M. H.; Barner-Kowollik, C.; Müller, A. H. E. Access to Cyclic Polystyrenes via a Combination of Reversible Addition Fragmentation Chain Transfer (RAFT) Polymerization and Click Chemistry. *Polymer* **2008**, *49* (9), 2274−2281.
(63) Laurent, B. A.; Grayson, S. M. An Efficient Route to Well-Defined Macrocyclic Polymers via "Click" Cyclization. *J. Am. Chem. Soc.* **2006**, *128* (13), 4238−4239.
(64) Nicolaÿ, R.; Matyjaszewski, K. Synthesis of Cyclic (Co)Polymers by Atom Transfer Radical Cross-Coupling and Ring Expansion by Nitroxide-Mediated Polymerization. *Macromolecules* **2011**, *44* (2), 240−247.
(65) Glassner, M.; Blinco, J. P.; Barner-Kowollik, C. Diels-Alder Reactions as an Efficient Route to High Purity Cyclic Polymers. *Macromol. Rapid Commun.* **2011**, *32* (9−10), 724−728.
(66) Liu, W.; Zhang, S.; Liu, S.; Wu, Z.; Chen, H. Efficient Heterodifunctional Unimolecular Ring-Closure Method for Cyclic

Polymers by Combining RAFT and SuFEx Click Reactions. *Macromol. Rapid Commun.* **2019**, *40* (20), 1900310.
(67) Bielawski, C. W.; Benitez, D.; Grubbs, R. H. An "Endless" Route to Cyclic Polymers. *Science (80-.)* **2002**, *297* (5589), 2041−2044.
(68) Gonsales, S. A.; Kubo, T.; Flint, M. K.; Abboud, K. A.; Sumerlin, B. S.; Veige, A. S. Highly Tactic Cyclic Polynorbornene: Stereoselective Ring Expansion Metathesis Polymerization of Norbornene Catalyzed by a New Tethered Tungsten-Alkylidene Catalyst. *J. Am. Chem. Soc.* **2016**, *138* (15), 4996−4999.
(69) Nadif, S. S.; Kubo, T.; Gonsales, S. A.; VenkatRamani, S.; Ghiviriga, I.; Sumerlin, B. S.; Veige, A. S. Introducing "Ynene" Metathesis: Ring-Expansion Metathesis Polymerization Leads to Highly Cis and Syndiotactic Cyclic Polymers of Norbornene. *J. Am. Chem. Soc.* **2016**, *138* (20), 6408−6411.
(70) Roland, C. D.; Li, H.; Abboud, K. A.; Wagener, K. B.; Veige, A. S. Cyclic Polymers from Alkynes. *Nat. Chem.* **2016**, *8* (8), 791−796.
(71) Wang, T. W.; Huang, P. R.; Chow, J. L.; Kaminsky, W.; Golder, M. R. A Cyclic Ruthenium Benzylidene Initiator Platform Enhances Reactivity for Ring-Expansion Metathesis Polymerization. *J. Am. Chem. Soc.* **2021**, *143* (19), 7314−7319.
(72) Mandal, U.; Ghiviriga, I.; Abboud, K. A.; Lester, D. W.; Veige, A. S. Double Tethered Metallacyclobutane Catalyst for Cyclic Polymer Synthesis. *J. Am. Chem. Soc.* **2021**, *143* (41), 17276−17283.
(73) Culkin, D. A.; Jeong, W.; Csihony, S.; Gomez, E. D.; Balsara, N. P.; Hedrick, J. L.; Waymouth, R. M. Zwitterionic Polymerization of Lactide to Cyclic Poly(Lactide) by Using N-Heterocyclic Carbene Organocatalysts. *Angew. Chem.* **2007**, *119* (15), 2681−2684.
(74) Shin, E. J.; Brown, H. A.; Gonzalez, S.; Jeong, W.; Hedrick, J. L.; Waymouth, R. M. Zwitterionic Copolymerization: Synthesis of Cyclic Gradient Copolymers. *Angew. Chemie - Int. Ed.* **2011**, *50* (28), 6388−6391.
(75) Stukenbroeker, T. S.; Solis-Ibarra, D.; Waymouth, R. M. Synthesis and Topological Trapping of Cyclic Poly(Alkylene Phosphates). *Macromolecules* **2014**, *47* (23), 8224−8230.
(76) Kammiyada, H.; Konishi, A.; Ouchi, M.; Sawamoto, M. Ring-Expansion Living Cationic Polymerization via Reversible Activation of a Hemiacetal Ester Bond. *ACS Macro Lett.* **2013**, *2* (6), 531−534.
(77) Kammiyada, H.; Ouchi, M.; Sawamoto, M. Ring-Expansion Living Cationic Polymerization of Vinyl Ethers: Optimized Ring Propagation. *Macromol. Symp.* **2015**, *350* (1), 105−116.
(78) Subramanian, G.; Shanbhag, S. Conformational Properties of Blends of Cyclic and Linear Polymer Melts. *Phys. Rev. E - Stat. Nonlinear, Soft Matter Phys.* **2008**, *77* (1), No. 011801.
(79) Vasquez, R.; Shanbhag, S. Percolation of Trace Amounts of Linear Polymers in Melts of Cyclic Polymers. *Macromol. Theory Simulations* **2011**, *20* (3), 205−211.
(80) Jacobson, H.; Stockmayer, W. H. Intramolecular Reaction in Polycondensations. I. The Theory of Linear Systems. *J. Chem. Phys.* **1950**, *18* (12), 1600.
(81) Jeong, Y.; Jin, Y.; Chang, T.; Uhlik, F.; Roovers, J. Intrinsic Viscosity of Cyclic Polystyrene. *Macromolecules* **2017**, *50* (19), 7770−7776.
(82) Ziebarth, J. D.; Gardiner, A. A.; Wang, Y.; Jeong, Y.; Ahn, J.; Jin, Y.; Chang, T. Comparison of Critical Adsorption Points of Ring Polymers with Linear Polymers. *Macromolecules* **2016**, *49* (22), 8780−8788.
(83) Parisi, D.; Kaliva, M.; Costanzo, S.; Huang, Q.; Lutz, P. J.; Ahn, J.; Chang, T.; Rubinstein, M.; Vlassopoulos, D. Nonlinear Rheometry of Entangled Polymeric Rings and Ring-Linear Blends. *J. Rheol. (N. Y. N. Y)* **2021**, *65* (4), 695−711.
(84) Barroso-Bujans, F.; Allgaier, J.; Alegria, A. Poly(Ethylene Oxide) Melt Intercalation in Graphite Oxide: Sensitivity to Topology, Cyclic versus Linear Chains. *Macromolecules* **2020**, *53* (1), 406−416.
(85) Lee, H. C.; Lee, H.; Lee, W.; Chang, T.; Roovers, J. Fractionation of Cyclic Polystyrene from Linear Precursor by HPLC at the Chromatographie Critical Condition. *Macromolecules* **2000**, *33* (22), 8119−8121.
(86) Takano, A.; Kushida, Y.; Aoki, K.; Masuoka, K.; Hayashida, K.; Cho, D.; Kawaguchi, D.; Matsushita, Y. HPLC Characterization of Cyclization Reaction Product Obtained by End-to-End Ring Closure Reaction of a Telechelic Polystyrene. *Macromolecules* **2007**, *40* (3), 679−681.
(87) Lepoittevin, B.; Dourges, M. A.; Masure, M.; Hemery, P.; Baran, K.; Cramail, H. Synthesis and Characterization of Ring-Shaped Polystyrenes. *Macromolecules* **2000**, *33* (22), 8218−8224.
(88) Lee, W.; Lee, H.; Lee, H. C.; Cho, D.; Chang, T.; Gorbunov, A. A.; Roovers, J. Retention Behavior of Linear and Ring Polystyrene at the Chromatographic Critical Condition. *Macromolecules* **2002**, *35* (2), 529−538.
(89) Dell, Z. E.; Schweizer, K. S. Intermolecular Structural Correlations in Model Globular and Unconcatenated Ring Polymer Liquids. *Soft Matter* **2018**, *14* (45), 9132−9142.
(90) Lang, M.; Fischer, J.; Sommer, J. U. Effect of Topology on the Conformations of Ring Polymers. *Macromolecules* **2012**, *45* (18), 7642−7648.
(91) Obukhov, S.; Johner, A.; Baschnagel, J.; Meyer, H.; Wittmer, J. P. Melt of Polymer Rings: The Decorated Loop Model. *EPL* **2014**, *105* (4), 48005.
(92) Rubinstein, M. Dynamics of Ring Polymers in the Presence of Fixed Obstacles. *Phys. Rev. Lett.* **1986**, *57* (24), 3023−3026.
(93) Sakaue, T. Statistics and Geometrical Picture of Ring Polymer Melts and Solutions. *Phys. Rev. E - Stat. Nonlinear, Soft Matter Phys.* **2012**, *85* (2), No. 021806.
(94) Suzuki, J.; Takano, A.; Deguchi, T.; Matsushita, Y. Dimension of Ring Polymers in Bulk Studied by Monte-Carlo Simulation and Self-Consistent Theory. *J. Chem. Phys.* **2009**, *131* (14), No. 144902.
(95) Ge, T.; Panyukov, S.; Rubinstein, M. Self-Similar Conformations and Dynamics in Entangled Melts and Solutions of Nonconcatenated Ring Polymers. *Macromolecules* **2016**, *49* (2), 708−722.
(96) Ubertini, M. A.; Smrek, J.; Rosa, A. Entanglement Length Scale Separates Threading from Branching of Unknotted and Non-Concatenated Ring Polymers in Melts. *Macromolecules* **2022**, *55*, 10723.
(97) Cremer, T.; Cremer, C. Chromosome Territories, Nuclear Architecture and Gene Regulation in Mammalian Cells. *Nat. Rev. Genet.* **2001**, *2* (4), 292−301.
(98) Rosa, A.; Everaers, R. Ring Polymers in the Melt State: The Physics of Crumpling. *Phys. Rev. Lett.* **2014**, *112* (11), No. 118302.
(99) Jeong, C.; Douglas, J. F. Relation between Polymer Conformational Structure and Dynamics in Linear and Ring Polyethylene Blends. *Macromol. Theory Simulations* **2017**, *26* (5), No. 1700045.
(100) Hur, K.; Jeong, C.; Winkler, R. G.; Lacevic, N.; Gee, R. H.; Yoon, D. Y. Chain Dynamics of Ring and Linear Polyethylene Melts from Molecular Dynamics Simulations. *Macromolecules* **2011**, *44* (7), 2311−2315.
(101) Tsalikis, D. G.; Alatas, P. V.; Peristeras, L. D.; Mavrantzas, V. G. Scaling Laws for the Conformation and Viscosity of Ring Polymers in the Crossover Region around Me from Detailed Molecular Dynamics Simulations. *ACS Macro Lett.* **2018**, *7* (8), 916−920.
(102) Reigh, S. Y.; Yoon, D. Y. Concentration Dependence of Ring Polymer Conformations from Monte Carlo Simulations. *ACS Macro Lett.* **2013**, *2* (4), 296−300.
(103) Zhang, T.; Winey, K. I.; Riggleman, R. A. Conformation and Dynamics of Ring Polymers under Symmetric Thin Film Confinement. *J. Chem. Phys.* **2020**, *153* (18), No. 184905.
(104) Terao, K.; Morihana, N.; Ichikawa, H. Solution SAXS Measurements over a Wide Temperature Range to Determine the Unperturbed Chain Dimensions of Polystyrene and a Cyclic Amylose Derivative. *Polym. J.* **2014**, *46* (3), 155−159.
(105) Arrighi, V.; Gagliardi, S.; Dagger, A. C.; Semlyen, J. A.; Higgins, J. S.; Shenton, M. J. Conformation of Cyclics and Linear Chain Polymers in Bulk by SANS. *Macromolecules* **2004**, *37* (21), 8057−8065.
(106) Debye, P. Light Scattering in Solutions. *J. Appl. Phys.* **1944**, *15* (4), 338−342.
(107) Gagliardi, S.; Arrighi, V.; Ferguson, R.; Dagger, A. C.; Semlyen, J. A.; Higgins, J. S. On the Difference in Scattering Behavior of Cyclic and Linear Polymers in Bulk. *J. Chem. Phys.* **2005**, *122* (6), No. 064904.
(108) Casassa, E. F. Some Statistical Properties of Flexible Ring Polymers. *J. Polym. Sci. Part A Gen. Pap.* **1965**, *3* (2), 605−614.

https://doi.org/10.1021/acs.macromol.3c00560
Macromolecules 2023, 56, 7203−7229

(109) Iwamoto, T.; Doi, Y.; Kinoshita, K.; Ohta, Y.; Takano, A.; Takahashi, Y.; Nagao, M.; Matsushita, Y. Conformations of Ring Polystyrenes in Bulk Studied by SANS. *Macromolecules* **2018**, *51* (4), 1539−1548.
(110) Kruteva, M.; Monkenbusch, M.; Pyckhout-Hintzen, W.; Allgaier, J.; Porcar, L.; Richter, D. Structure of Polymer Rings in Linear Matrices: SANS Investigation. *Macromolecules* **2023**, *56* (13), 4835−4844.
(111) Bensafi, A.; Maschke, U.; Benmouna, M. Cyclic Polymers in Good Solvents. *Polym. Int.* **2000**, *49* (2), 175−183.
(112) Takano, A.; Kushida, Y.; Ohta, Y.; Masuoka, K.; Matsushita, Y. The Second Virial Coefficients of Highly-Purified Ring Polystyrenes in Cyclohexane. *Polymer (Guildf)* **2009**, *50* (5), 1300−1303.
(113) Moore, N. T.; Grosberg, A. Y. Limits of Analogy between Self-Avoidance and Topology-Driven Swelling of Polymer Loops. *Phys. Rev. E - Stat. Nonlinear, Soft Matter Phys.* **2005**, *72* (6), No. 061803.
(114) Iyer, B. V. S.; Lele, A. K.; Shanbhag, S. What Is the Size of a Ring Polymer in a Ring-Linear Blend? *Macromolecules* **2007**, *40* (16), 5995−6000.
(115) Subramanian, G.; Shanbhag, S. Self-Diffusion in Binary Blends of Cyclic and Linear Polymers. *Macromolecules* **2008**, *41* (19), 7239−7242.
(116) Sakaue, T.; Nakajima, C. H. Miscibility Phase Diagram of Ring-Polymer Blends: A Topological Effect. *Phys. Rev. E* **2016**, *93* (4), No. 042502.
(117) Tsalikis, D. G.; Koukoulas, T.; Mavrantzas, V. G. Dynamic, Conformational and Topological Properties of Ring−Linear Poly(Ethylene Oxide) Blends from Molecular Dynamics Simulations. *React. Funct. Polym.* **2014**, *80*, 61−70.
(118) Hagita, K.; Murashima, T. Molecular Dynamics Simulations of Ring Shapes on a Ring Fraction in Ring-Linear Polymer Blends. *Macromolecules* **2021**, *54* (17), 8043−8051.
(119) Iwamoto, T.; Doi, Y.; Kinoshita, K.; Takano, A.; Takahashi, Y.; Kim, E.; Kim, T. H.; Takata, S. I.; Nagao, M.; Matsushita, Y. Conformations of Ring Polystyrenes in Semidilute Solutions and in Linear Polymer Matrices Studied by SANS. *Macromolecules* **2018**, *51* (17), 6836−6847.
(120) Grest, G. S.; Ge, T.; Plimpton, S. J.; Rubinstein, M.; O'Connor, T. C. Entropic Mixing of Ring/Linear Polymer Blends. *ACS Polym. Au* **2023**, *3* (2), 209−216.
(121) Smrek, J.; Chubak, I.; Likos, C. N.; Kremer, K. Active Topological Glass. *Nat. Commun.* **2020**, *11* (1), 1−11.
(122) Soh, B. W.; Klotz, A. R.; Robertson-Anderson, R. M.; Doyle, P. S. Long-Lived Self-Entanglements in Ring Polymers. *Phys. Rev. Lett.* **2019**, *123* (4), No. 048002.
(123) Regan, K.; Ricketts, S.; Robertson-Anderson, R. DNA as a Model for Probing Polymer Entanglements: Circular Polymers and Non-Classical Dynamics. *Polymers (Basel)* **2016**, *8* (9), 336.
(124) Staňo, R.; Likos, C. N.; Smrek, J. To Thread or Not to Thread? Effective Potentials and Threading Interactions between Asymmetric Ring Polymers. *Soft Matter* **2022**, *19* (1), 17−30.
(125) Obukhov, S. P.; Rubinstein, M.; Duke, T. Dynamics of a Ring Polymer in a Gel. *Phys. Rev. Lett.* **1994**, *73* (9), 1263−1266.
(126) Malo de Molina, P.; Alegría, A.; Allgaier, J.; Kruteva, M.; Hoffmann, I.; Prévost, S.; Monkenbusch, M.; Richter, D.; Arbe, A.; Colmenero, J. Direct Observation of Dynamic Tube Dilation in Entangled Polymer Blends: A Combination of Neutron Scattering and Dielectric Techniques. *Phys. Rev. Lett.* **2019**, *123* (18), No. 187802.
(127) Gold, B. J.; Pyckhout-Hintzen, W.; Wischnewski, A.; Radulescu, A.; Monkenbusch, M.; Allgaier, J.; Hoffmann, I.; Parisi, D.; Vlassopoulos, D.; Richter, D. Direct Assessment of Tube Dilation in Entangled Polymers. *Phys. Rev. Lett.* **2019**, *122* (8), No. 088001.
(128) Halverson, J. D.; Lee, W. B.; Grest, G. S.; Grosberg, A. Y.; Kremer, K. Molecular Dynamics Simulation Study of Nonconcatenated Ring Polymers in a Melt. II. Dynamics. *J. Chem. Phys.* **2011**, *134* (20), No. 204905.
(129) Pasquino, R.; Vasilakopoulos, T. C.; Jeong, Y. C.; Lee, H.; Rogers, S.; Sakellariou, G.; Allgaier, J.; Takano, A.; Brás, A. R.; Chang, T.; Gooßen, S.; Pyckhout-Hintzen, W.; Wischnewski, A.; Hadjichristidis, N.; Richter, D.; Rubinstein, M.; Vlassopoulos, D. Viscosity of Ring Polymer Melts. *ACS Macro Lett.* **2013**, *2* (10), 874−878.
(130) Tsalikis, D. G.; Koukoulas, T.; Mavrantzas, V. G.; Pasquino, R.; Vlassopoulos, D.; Pyckhout-Hintzen, W.; Wischnewski, A.; Monkenbusch, M.; Richter, D. Microscopic Structure, Conformation, and Dynamics of Ring and Linear Poly(Ethylene Oxide) Melts from Detailed Atomistic Molecular Dynamics Simulations: Dependence on Chain Length and Direct Comparison with Experimental Data. *Macromolecules* **2017**, *50* (6), 2565−2584.
(131) Wong, C. P. J.; Choi, P. On the Diffusivity of Ring Polymers. *Soft Matter* **2020**, *16* (9), 2350−2362.
(132) Michieletto, D.; Sakaue, T. Dynamical Entanglement and Cooperative Dynamics in Entangled Solutions of Ring and Linear Polymers. *ACS Macro Lett.* **2021**, *10* (1), 129−134.
(133) Rubinstein, M.; Colby, R. H. *Polymer Physics*; Oxford University Press: Oxford, 2003.
(134) Brás, A. R.; Pasquino, R.; Koukoulas, T.; Tsolou, G.; Holderer, O.; Radulescu, A.; Allgaier, J.; Mavrantzas, V. G.; Pyckhout-Hintzen, W.; Wischnewski, A.; Vlassopoulos, D.; Richter, D. Structure and Dynamics of Polymer Rings by Neutron Scattering: Breakdown of the Rouse Model. *Soft Matter* **2011**, *7* (23), 11169.
(135) Brás, A. R.; Goossen, S.; Krutyeva, M.; Radulescu, A.; Farago, B.; Allgaier, J.; Pyckhout-Hintzen, W.; Wischnewski, A.; Richter, D. Compact Structure and Non-Gaussian Dynamics of Ring Polymer Melts. *Soft Matter* **2014**, *10* (20), 3649−3655.
(136) Gooßen, S.; Krutyeva, M.; Sharp, M.; Feoktystov, A.; Allgaier, J.; Pyckhout-Hintzen, W.; Wischnewski, A.; Richter, D. Sensing Polymer Chain Dynamics through Ring Topology: A Neutron Spin Echo Study. *Phys. Rev. Lett.* **2015**, *115* (14), No. 148302.
(137) Guenza, M. G. Localization of Chain Dynamics in Entangled Polymer Melts. *Phys. Rev. E - Stat. Nonlinear, Soft Matter Phys.* **2014**, *89* (5), No. 052603.
(138) Arrighi, V.; Gagliardi, S.; Ganazzoli, F.; Higgins, J. S.; Raffaini, G.; Tanchawanich, J.; Taylor, J.; Telling, M. T. F. Effect of Chain Length and Topological Constraints on Segmental Relaxation in Cyclic PDMS. *Macromolecules* **2018**, *51* (18), 7209−7223.
(139) Arrighi, V.; Ganazzoli, F.; Zhang, C.; Gagliardi, S. New Interpretation of Local Dynamics of Poly(Dimethyl Siloxane) Observed by Quasielastic Neutron Scattering. *Phys. Rev. Lett.* **2003**, *90* (5), 4.
(140) Mills, P. J.; Mayer, J. W.; Kramer, E. J.; Hadziioannou, G.; Lutz, P.; Strazielle, C.; Rempp, P.; Kovacs, A. J. Diffusion of Polymer Rings in Linear Polymer Matrices. *Macromolecules* **1987**, *20* (3), 513−518.
(141) Geyler, S.; Pakula, T. Conformation of Ring Polymers in Computer Simulated Melts. *Die Makromol. Chemie, Rapid Commun.* **1988**, *623* (9), 617−623.
(142) McKenna, G. B.; Plazek, D. J. Viscosity of Blends of Linear and Cyclic Molecules of Similar Molecular Mass. *Polym. Commun. Guildf.* **1986**, *27* (10), 304−306.
(143) Papadopoulos, G. D.; Tsalikis, D. G.; Mavrantzas, V. G. Microscopic Dynamics and Topology of Polymer Rings Immersed in a Host Matrix of Longer Linear Polymers: Results from a Detailed Molecular Dynamics Simulation Study and Comparison with Experimental Data. *Polymers (Basel)* **2016**, *8* (8), 283.
(144) Klein, J. Dynamics of Entangled Linear, Branched, and Cyclic Polymers. *Macromolecules* **1986**, *19* (1), 105−118.
(145) Kärger, J. Zur Bestimmung Der Diffusion in Einem Zweibereichsystem Mit Hilfe von Gepulsten Feldgradienten. *Ann. Phys.* **1969**, *479* (1−2), 1−4.
(146) Kärger, J. Der Einfluß Der Zweibereichdiffusion Auf Die Spinechodämpfung Unter Berücksichtigung Der Relaxation Bei Messungen Mit Der Methode Der Gepulsten Feldgradienten. *Ann. Phys.* **1971**, *482* (1), 107−109.
(147) Tsalikis, D. G.; Mavrantzas, V. G. Size and Diffusivity of Polymer Rings in Linear Polymer Matrices: The Key Role of Threading Events. *Macromolecules* **2020**, *53* (3), 803−820.
(148) Shaffer, J. S. Effects of Chain Topology on Polymer Dynamics: Bulk Melts. *J. Chem. Phys.* **1994**, *101* (5), 4205.

https://doi.org/10.1021/acs.macromol.3c00560
Macromolecules 2023, 56, 7203−7229

(149) Mo, J.; Wang, J.; Wang, Z.; Lu, Y.; An, L. Size and Dynamics of a Tracer Ring Polymer Embedded in a Linear Polymer Chain Melt Matrix. *Macromolecules* **2022**, *55* (5), 1505−1514.
(150) Parisi, D.; Ahn, J.; Chang, T.; Vlassopoulos, D.; Rubinstein, M. Stress Relaxation in Symmetric Ring-Linear Polymer Blends at Low Ring Fractions. *Macromolecules* **2020**, *53* (5), 1685−1693.
(151) O'Connor, T. C.; Ge, T.; Grest, G. S. Composite Entanglement Topology and Extensional Rheology of Symmetric Ring-Linear Polymer Blends. *J. Rheol. (N. Y. N. Y)* **2022**, *66* (1), 49−65.
(152) Cremer, T.; Cremer, M.; Dietzel, S.; Müller, S.; Solovei, I.; Fakan, S. Chromosome Territories—A Functional Nuclear Landscape. *Curr. Opin. Cell Biol.* **2006**, *3*, 307−316.
(153) Jun, S.; Mulder, B. Entropy-Driven Spatial Organization of Highly Confined Polymers: Lessons for the Bacterial Chromosome. *Proc. Natl. Acad. Sci. U. S. A* **2006**, *103* (33), 12388−12393.
(154) Michieletto, D.; Marenduzzo, D.; Orlandini, E.; Alexander, G. P.; Turner, M. S. Threading Dynamics of Ring Polymers in a Gel. *ACS Macro Lett.* **2014**, *3* (3), 255−259.
(155) Gibbs, J. H.; DiMarzio, E. A. Nature of the Glass Transition and the Glassy State. *J. Chem. Phys.* **1958**, *28* (3), 373−383.
(156) Michieletto, D.; Nahali, N.; Rosa, A. Glassiness and Heterogeneous Dynamics in Dense Solutions of Ring Polymers. *Phys. Rev. Lett.* **2017**, *119* (19), No. 197801.
(157) Li, J.; Zhang, B.; Li, Y. Glass Formation in Mechanically Interlocked Ring Polymers: The Role of Induced Chain Stiffness. *Macromolecules* **2022**, *56* (2), 589−600.
(158) Mei, B.; Dell, Z. E.; Schweizer, K. S. Microscopic Theory of Long-Time Center-of-Mass Self-Diffusion and Anomalous Transport in Ring Polymer Liquids. *Macromolecules* **2020**, *53* (23), 10431−10445.
(159) Likos, C. N.; Löwen, H.; Watzlawek, M.; Abbas, B.; Jucknischke, O.; Allgaier, J.; Richter, D. Star Polymers Viewed as Ultrasoft Colloidal Particles. *Phys. Rev. Lett.* **1998**, *80* (20), 4450.
(160) Salez, T.; Salez, J.; Dalnoki-Veress, K.; Raphaël, E.; Forrest, J. A. Cooperative Strings and Glassy Interfaces. *Proc. Natl. Acad. Sci. U. S. A* **2015**, *112* (27), 8227−8231.
(161) Mirigian, S.; Schweizer, K. S. Elastically Cooperative Activated Barrier Hopping Theory of Relaxation in Viscous Fluids.I.General Formulation and Application to Hard Sphere Fluids. *J. Chem. Phys.* **2014**, *140* (19), No. 194506.
(162) Mei, B.; Zhou, Y.; Schweizer, K. S. Thermodynamics-Structure-Dynamics Correlations and Nonuniversal Effects in the Elastically Collective Activated Hopping Theory of Glass-Forming Liquids. *J. Phys. Chem. B* **2020**, *124* (28), 6121−6131.
(163) Schweizer, K. S.; Saltzman, E. J. Entropic Barriers, Activated Hopping, and the Glass Transition in Colloidal Suspensions. *J. Chem. Phys.* **2003**, *119* (2), 1181−1196.
(164) Mirigian, S.; Schweizer, K. S. Elastically Cooperative Activated Barrier Hopping Theory of Relaxation in Viscous Fluids. II. Thermal Liquids. *J. Chem. Phys.* **2014**, *140* (19), No. 194507.
(165) Phan, A. D.; Schweizer, K. S. Theory of Activated Glassy Dynamics in Randomly Pinned Fluids. *J. Chem. Phys.* **2018**, *148* (5), No. 054502.
(166) Jun, S.; Mulder, B. Entropy-Driven Spatial Organization of Highly Confined Polymers: Lessons for the Bacterial Chromosome. *Proc. Natl. Acad. Sci. U. S. A.* **2006**, *103* (33), 12388−12393.

https://doi.org/10.1021/acs.macromol.3c00560
Macromolecules 2023, 56, 7203−7229